European Journal of Medicinal Chemistry 125 (2017) 255–268

Contents lists available at ScienceDirect

European Journal of Medicinal Chemistry

journal homepage: http://www.elsevier.com/locate/ejmech

Research paper

Synthesis and evaluation of C9 alkoxy analogues of (-)-stepholidine as dopamine receptor ligands

Sudharshan Madapa [a], Satishkumar Gadhiya [a, b], Thomas Kurtzman [b, c, d], Ian L. Alberts [e], Steven Ramsey [c, d], Maarten Reith [f], Wayne W. Harding [a, b, c, *]

[a] Department of Chemistry, Hunter College, City University of New York, 695 Park Avenue, NY 10065, USA
[b] Ph.D. Program in Chemistry, CUNY Graduate Center, 365 5th Avenue, New York, NY 10016, USA
[c] Ph.D. Program in Biochemistry, CUNY Graduate Center, 365 5th Avenue, New York, NY 10016, USA
[d] Department of Chemistry, Lehman College, The City University of New York, Bronx, NY 10468, USA
[e] Department of Natural Sciences, LaGuardia Community College, City University of New York, New York, NY 11101, USA
[f] Department of Psychiatry, New York University, New York, NY 10016, USA

ARTICLE INFO

Article history:
Received 11 July 2016
Received in revised form
9 September 2016
Accepted 10 September 2016
Available online 14 September 2016

Keywords:
Dopamine
D1
D3
Tetrahydroprotoberberine
THPB
Stepholidine

ABSTRACT

Tetrahydroprotoberberine alkaloids have shown interesting polypharmacological actions at dopamine receptors and are a unique template from which to mine novel molecules with dual selective actions at D1 and D3 receptors. Such compounds will be valuable to evaluate as anti-cocaine therapeutics. Towards that eventual goal, we engaged an SAR study in which a series of C9 alkoxy analogues of the D1/D2/D3 ligand (-)-stepholidine that possessed or lacked a C12 bromo functionality, were synthesized and evaluated for affinity at dopamine D1, D2 and D3 receptors. We found that the analogues are generally selective for the D1 receptor. Small n-alkoxy substituents (up to 4 carbons in length) were generally well tolerated for high D1 affinity but such groups reduced D3 affinity. In the case of C12 brominated analogues, C9 alkoxylation also had little effect on D1 affinity for the smaller alkoxy groups, but reduced D2 and D3 affinities significantly. C12 bromination tends to increase D1 receptor selectivity. A number of compounds were identified that retain affinity for D1 and D3 receptors but lack D2 receptor affinity. Among them, compound 22a was found to be a selective D1/D3 dual antagonist (Ki = 5.3 and 106 nM at D1 and D3 receptors). Docking studies performed on the analogues at the D3 receptor revealed a number of interactions that are important for affinity including a critical N - Asp110 salt bridge motif, H-bonds to Ser192 and Cys181 and hydrophobic interactions between the aryl rings and Phe106 and Phe345. The analogues adopt an orientation in which ring A is located in the orthosteric binding site while the C9 alkoxy substituents attached to ring D project into the secondary binding pocket of the D3 receptor.

1. Introduction

The interesting central nervous system (CNS) receptor pharmacology exhibited by members of the tetrahydroprotoberberine (THPB) class of alkaloids, has led to a number of synthetic and biological explorations on the scaffold. Naturally occurring THPBs as well as synthetic derivatives have shown activity at D1 and D2 receptors and are promising lead compounds for the development of therapeutics to treat a range of neuropsychiatric disorders and drug abuse [1,2]. For example, stepholidine (**1**, Fig. 1) displays a very rare D1 agonist/D2 antagonist/D3 antagonist profile and possesses antipsychotic, memory enhancing and anti-addiction properties [3–12]. Isocorypalmine (**2**) is a D1 partial agonist/D2 antagonist/D3 antagonist that has been shown to reduce cocaine reinstatement [13]. Tetrahydropalmatine (**3**) is a D1/D2 antagonist with potential as an anti-addiction therapeutic [13–20]. Govadine (**4**) has cognitive enhancement properties which have been attributed to antagonist activity at D1 and D2 receptors [21–24]. The synthetic THPB 12-chloroscoulerine (**5**) displays D1 agonist/D2 antagonist activity and potent antipsychotic properties [25–27]. Overall, it appears that the dopamine receptor polypharmacology of THPBs is relevant to their central nervous system (CNS) therapeutic potential.

A number of SAR studies have been performed on the THPB

* Corresponding author. Department of Chemistry, Hunter College, City University of New York, 695 Park Avenue, NY 10065, USA.
E-mail address: whardi@hunter.cuny.edu (W.W. Harding).

http://dx.doi.org/10.1016/j.ejmech.2016.09.036
0223-5234/

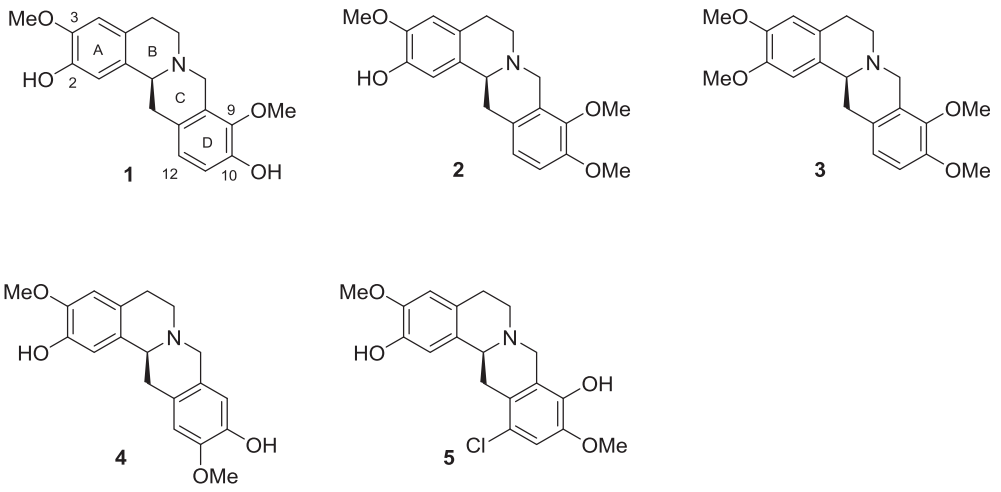

Fig. 1. Structures of THPBS: stepholidine (**1**), isocorypalmine (**2**), tetrahydropalmatine (**3**), govadine (**4**), 12-chloroscoulerine (**5**).

template previously which have indicated that the placement and identity of substituents on the aryl rings of THPBs can significantly influence affinity and activity of the compounds at dopamine D1 and D2 receptors [1,2,28–30]. We considered the possibility that the THPB scaffold could provide a source for novel compounds with potent polypharmacological activities at dopamine receptors. We are particularly interested in obtaining compounds that possess selective, dual D1/D3 activity (but lacking D2 affinity) as such compounds will be useful as tools to further probe the effects of multiple receptor modulation in the treatment of substance abuse disorders. As blockade of D2 receptors is associated with motoric side effects we envisage that selective dual D1/D3 agents will have a lower propensity to produce such side effects. In light of these promising outcomes, we engaged an SAR study as part of a longer term strategy to use THPBs to acquire new pharmacological tools and drugs relevant to substance abuse disorders. This report describes synthetic, biological and computational experiments in this direction.

2. Results and discussion

2.1. Synthesis

As alluded to before several THPBs (natural and synthetic) have been evaluated at D1 and D2 receptors and promising activities have been discovered for a number of compounds which therefore makes the THPB template a valuable and interesting subject of synthetic and medicinal chemistry studies. We chose stepholidine (**1**) as the lead compound for this study. Data from the Psychoactive Drug Screening Program (PDSP) indicates that **1** has affinity for D1, D2 and D3 receptors with K_i values of 5.9, 974 and 30 nM respectively. Prior SAR work on stepholidine suggests an important role for the C2 and C10 phenolic groups for affinity at D1 and D2 receptors [2]. Indeed the phenolic groups of THPBs are generally recognized as being very important for affinity at D1 and D2 receptors and the placement of oxygenated groups on the template can impact D1/D2 selectivity as well. For example coreximine, an isomer of **1** that contains a C11 methoxy group rather than the C9 methoxy group of stepholidine, is selective for the D2 receptor (i.e in contrast to **1** which is D1 selective) [30]. Although some D1 and D2 receptor binding studies have been performed on THPBs in general and on stepholidine in particular, there have been no prior SAR studies investigating the tolerance for substituents at the C9 position of stepholidine with respect to D1 and D2 affinities. Furthermore, there is a paucity of SAR information concerning the impact of structural modification of THPBs in general (including stepholidine) in relation to affinity and activity at D3 receptors [31]. Halogen atoms can provide significant gains in receptor affinity to a scaffold [32]. Although the presence of a C12 chloro group affords high D1 receptor affinity in the case of 12-chloroscoulerine (**5**), the effect of the presence of a bromo group at C12 of stepholidine analogues on D1, D2 and D3 affinity, has not been assessed up to now. Thus to illuminate these aspects of the SARs of THPBs in general and stepholidine in particular, we focused our study on the C9 and C12 positions.We targeted the preparation of a series of C9 alkoxy analogues as these compounds would help to elucidate the steric tolerance at this position for dopamine receptor affinities. The addition of a C12 bromine atom to the aforementioned compounds would reveal whether bromination at C12 may enhance dopamine receptor affinities and the extent to which this was generalizable for parallel series of compounds. We envisaged that the synthesis of the C9 alkoxy/C12 bromo analogues could be effected via a brominated 1,2,4,5-tetrasubstituted phenylacetic acid intermediate (**13**, Scheme 1). This intermediate would eventually be transformed into the ring D moiety in the analogues [33]. Removal of the bromo group from the C9 alkoxy/C12 bromo analogues would afford the desired, analogous C9 alkoxy compounds.

Preparation of the tetrasubstituted intermediate (**13**) commenced with 3,4-dihydroxybenzaldehyde (**6**) as shown in Scheme 1. Selective benzylation of the 4-hydroxyl group of **6** gave aldehyde **7**. The phenolic group of **7** was then protected to give silyl ether **8**. This was followed by bromination to afford aldehyde **9**, which was then reduced to give alcohol **10**. Compound **10** was converted to the dibromide **11** by reaction with PBr_3. The primary bromide group of **11** was displaced by cyanide ion and the resulting nitrile (**12**) was hydrolyzed under basic conditions (resulting in concomitant removal of the silyl protecting group) to give acid **13**.

Scheme 2 shows the preparation of the THPB framework and subsequent functionalization to afford the two series of analogues (the brominated series, **20a**–**g** and the non-brominated series, **22a**–**g**). Thus, acid **13** was coupled with readily available amine **14** and the amide **15** thus formed was cyclized under Bischler-Napieralski conditions to give **16**. The dihydroisoquinoline **16** was reduced via Noyori's method providing the benzyltetrahydroisoquinoline **17**. Compound **17** was heated with formalin promoting Mannich cyclization to form the tetracyclic THPB skeleton in **18**. Alkylation of the C9 phenolic group of **18** gave the C12 bromo/C9 alkoxy intermediates **19a**–**g**. The benzyl groups of the

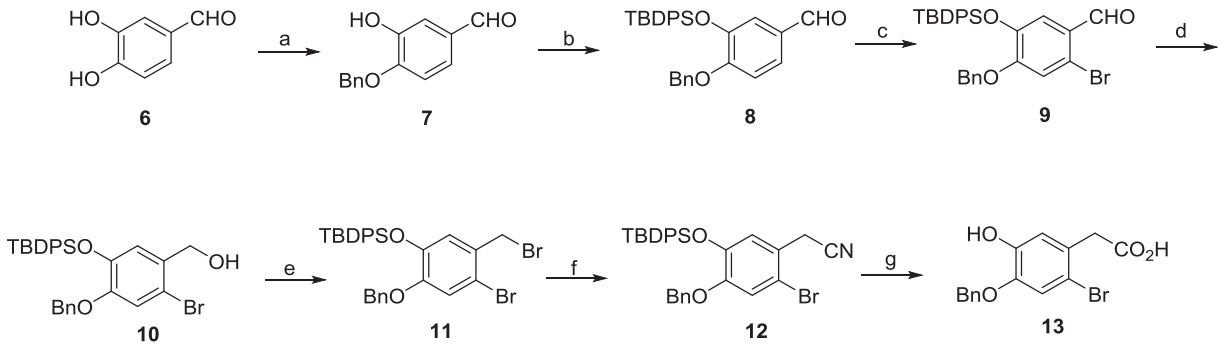

Scheme 1. *Reagents and conditions*: (a) K_2CO_3, ACN, reflux, 2 h, 75%; (b) TEA, DMAP, TBDPSCl, DCM, 10 h; (c) Br_2, MeOH, 1 h, 85% from **7**; (d) $NaBH_4$, MeOH, 1 h, 93%; (e) PBr_3, DCM, 2 h, 82%; (f) NaCN, DMF, 3h, 75%; (g) NaOH, EtOH, H_2O, 75 °C, 5h, 81%.

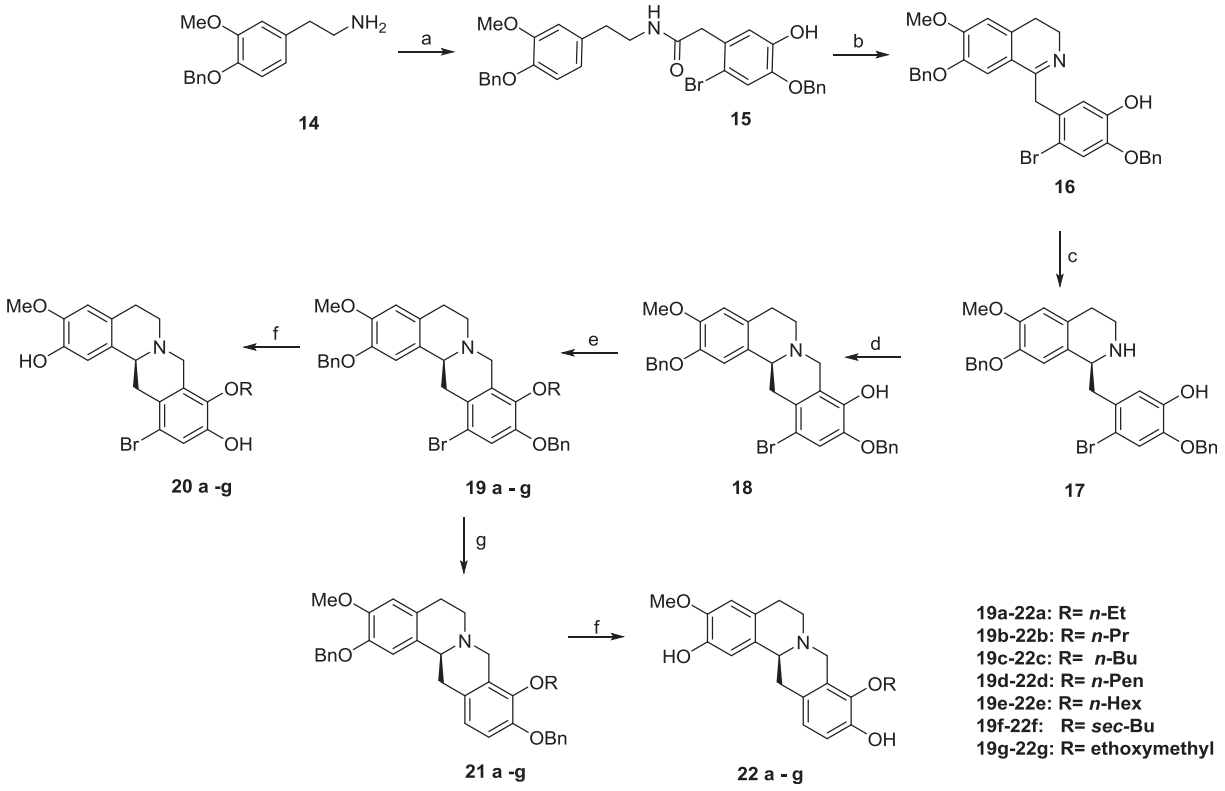

Scheme 2. *Reagents and conditions*: (a) EDC, DMF, **13**, 12 h, 43%; (b) $POCl_3$, ACN, 70 °C, 1 h; (c) Noyori catalyst, DMF, HCOOH/TEA (5/2), 12 h, 40% from **15**; (d) formalin, MeOH, 90 °C, 3 h, 63%; (e) appropriate alkyl halide, K_2CO_3, DMF, 2–4 h, 64–82%; (f) conc. HCl, EtOH, 70 °C, 1.5–2 h, 58–81%.for **20a**–**g**; (g) *i*-PrMgCl, LiCl, THF, 0 °C, 2 h.

intermediates **19a**–**g** were subsequently removed by treatment with concentrated HCl to give brominated analogues **20a**–**g**. The corresponding C9 alkoxy analogues (**22a**–**g**) were prepared from **19a**–**g** by treatment with *i*-PrMgCl (to remove the bromo group; compounds **21a**–**g**), followed by treatment with concentrated HCl to effect debenzylation as before.

2.2. Biological evaluations

2.2.1. Binding affinity at D1, D2 and D3 receptors

Compounds **20a**–**20g** and **22a**–**22g** were assayed for binding affinity to human dopamine D1, D2 and D3 receptors by the Psychoactive Drug Screening Program (PDSP). Details of the screening protocol may be found online at the PDSP website (https://pdspdb.unc.edu/pdspWeb/). In brief, the compounds were initially assayed in quadruplicate at a 10 μM concentration at D1, D2, and D3 receptors. Compounds that showed an inhibition of binding of >50% were progressed to secondary assays to measure K_i. The K_i determinations were performed via 12-point concentration-response curves in triplicate (unless noted otherwise). This data is presented in Table 1.

2.2.1.1. SAR at the D1 receptor. At the D1 receptor, small C9 alkoxy groups were tolerated in the **20a**–**20g** series of compounds. In fact, the C9 ethoxy (**20a**), *n*-propyloxy (**20b**) and *n*-butyloxy (**20c**) compounds had the highest D1 receptor affinities of all compounds evaluated (K_i values of 1.3, 2.2 and 2.3 nM respectively). The methoxyethyl derivative **20g** also had strong D1 receptor affinity (4.2 nM). When compared to **20c** (which bears a similar length of atoms), this result tends to suggest that lipophilicity of the C9 substituent group *per se* is not a major contributor to affinity; perhaps steric effects are the major factors here. Alternatively, the

Table 1
Binding assay data (K_i in nM) for C9 analogues at dopamine D1, D2 and D3 receptors.

Compound	R^1	R^2	K_i (nM)[a]		
			D1[b]	D2[c]	D3[d]
20a	Et	Br	1.3 ± 0.2	NA[e]	373 ± 48
20b	*n*-Pr	Br	2.2 ± 0.3	70 ± 9.0	195 ± 25
20c	*n*-Bu	Br	2.3 ± 0.3	107 ± 14	>10, 000
20d	*n*-Pen	Br	32 ± 4.1	398 ± 51	3605 ± 470
20e	*n*-Hex	Br	68 ± 8.8	731 ± 94	3171 ± 410
20f	*sec*-Bu	Br	9.7 ± 1.3	331 ± 43	2070 ± 270
20g	Methoxyethyl	Br	4.2 ± 0.5	NA	726 ± 94
22a	Et	H	5.3 ± 0.7	NA	106 ± 14
22b	*n*-Pr	H	12 ± 1.5	41 ± 5.3	175 ± 23
22c	*n*-Bu	H	11 ± 1.4	NA	131 ± 17
22d	*n*-Pen	H	31 ± 4.0	23 ± 3.0	3213 ± 410
22e	*n*-Hex	H	77 ± 9.9	NA	195 ± 25
22f	*sec*-Bu	H	65 ± 8.4	104 ± 13	450 ± 58
22g	Methoxyethyl	H	7.7 ± 1.0	18 ± 2.3	31 ± 4.0
1[f]	Me	H	5.9	974	30

[a] Experiments carried out in triplicate - SEM values reported.
[b] [3H]SCH23390 used as radioligand.
[c] [3H]N-methylspiperone used as radioligand.
[d] [3H]N-methylspiperone used as radioligand.
[e] NA-not active (<50% inhibition in primary assay).
[f] Data from the PDSP online database.

additional oxygen atom in the alkyl chain of **20g** may be making significant H-bond contacts to overcome desolvation penalties upon binding to the receptor. The *n*-pentyloxy and *n*-hexyloxy analogues (**20d** and **20e** respectively) showed diminished D1 receptor affinities as compared to the smaller homologues. The *sec*-butyloxy analogue **20f** (a mixture of diastereomers) also displayed strong D1 receptor affinity (9.7 nM). Thus branching in the pendant alkyl chain does not seem to negatively impact D1 receptor affinity in a major way.

In the case of the **22a**–**22g** series of analogues, a similar trend as that obtained for the **20a**–**20g** series was observed wherein the analogues with smaller *n*-alkoxy groups (**22a**–**22c**) and the methoxyethyl analogue (**22g**) showed the highest D1 affinity in the series. The **22a**–**22c** subset of compounds, when compared to their C12 bromo counterparts (**20a**–**20c**), showed slightly diminished D1 receptor affinities (approximately 4–5 fold). The C9 sec-butyloxy analogue also showed reduced affinity (i.e. **22f** versus **20f**; approximately 7-fold). However, the affinities of the larger *n*-homologues (**22d** and **22e**) and the methoxyethyl analogue (**22g**) was similar to that of the corresponding C12 bromo analogues.

A recent study has noted the importance of the C9 oxygenated substituent in THPBs wherein a hydroxyl group at C9 engendered higher D1 and D2 receptor affinities than isomers in which the hydroxyl group is positioned at C11 instead [28,34]. Also, the presence of a C11 methoxyl group afforded higher dopamine receptor affinities than the comparable C11 hydroxy analogues. Thus, the position of phenolic and methoxyl groups in ring D can be very critical for D1 and D2 receptor affinities.

2.2.1.2. SAR at the D2 receptor. For the brominated series of compounds at the D2 receptor, there was a decrease in affinity as the length of the *n*-alkoxyl chain was extended from 3 to 6 carbon atoms (i.e. compounds **20b**–**20e**). Compounds **20a** and **20g** did not show any appreciable D2 receptor affinity in the primary assay and were not evaluated in the secondary assay. The affinities of the brominated group of compounds for the D2 receptor was significantly lower (>10-fold) than that for the D1 receptor for all compounds tested.

No clear trend could be discerned for the **22a**–**22g** set of compounds at the D2 receptor and some compounds lacked any appreciable affinity from the primary assay (specifically **22a**, **22c** and **22e**). Compound **22g** when compared with butyloxy analogue **22c**, showed improved D2 receptor affinity which suggests that the additional oxygen atom in **22g** makes important binding contacts with the D2 receptor. This was a reversal in the trend that was observed with comparable compounds in the brominated series (i.e. compound **20c** – 107 nM versus compound **20g** – no activity). In general, the D2 receptor affinities for this group was lower than their D1 receptor affinities. Our work demonstrates that a 9-alkoxy, 10-hydroxy substitution pattern in ring D tends to favor selectivity for the D1 receptor and depending on the particular C9 alkoxy substituent, may decimate D2 receptor affinity.

2.2.1.3. SAR at the D3 receptor. At the D3 receptor, no clear trend was seen for either the brominated or non-brominated series of compounds. For the brominated group, most compounds (save for **20a**) had lower affinity for the D3 receptor as compared to D2 and D1 receptors. Methoxyethyl analogue **22g** had a 4-fold higher affinity than the *n*-butyloxy analogue **22c**, indicating that perhaps the extra oxygen atom in **22g** makes favorable D3 receptor contacts. All compounds assessed showed decreased D3 receptor affinity as compared to the lead compound stepholidine, except for compound **22g** which showed similar D3 receptor affinity. In general, the absence of a C12 bromo group improves D3 receptor affinity (e.g. compare **22g** versus **20g**; 31 nM versus 726 nM respectively).

2.2.2. Evaluation of functional activity

We were pleased to find that a number of compounds displayed the extremely unusual binding profile that we desired, in that they had affinity for D1 and D3 receptors but lacked affinity for D2 receptors. Since compound **22a** had the highest D3 affinity among all such compounds, we decided to further characterize the functional activity of this compound at D1 and D3 receptors as a representative of the series. In these assays compound **22a** lacked intrinsic activity at D1 and D3 receptors (as measured by its inability to stimulate binding of GTPγ-S as opposed to the activation caused by dopamine), indicating that the compound is not an agonist at either receptor. A follow-up D1 Tango antagonist assay at the PDSP revealed that **22a** is in fact a D1 antagonist (IC_{50} = 416 nM; IC_{50} of the standard SCH 23390 at D1 in this assay was 2.4 nM). Compound **22a** is a dopamine D3 antagonist; it caused a dextral shift in the curve for dopamine in stimulating GTPγ-S binding to cells heterologously expressing the D3 receptor with a K_e of 3.15 nM.

2.3. D3 receptor docking studies

The analogues evaluated in this study generally exhibit high affinity and selectivity for the D1 receptor with low to moderate D3 affinity. As we were interested in obtaining compounds with high D3 affinity, we decided to dock the analogues at the D3 receptor as this could provide important revelations as to the receptor-ligand interactions that impact D3 affinity and thus facilitate future pharmacodynamic optimization. For these docking simulations, we prepared a target structure for the D3 receptor based on the X-ray crystal structure with PDB code 3PBL and resolution 2.89 Å [35]. The 3PBL receptor structure was obtained from the Protein Data Bank (www.rcsb.org) [36] and prepared for the modeling simulations by application of the Protein Preparation Wizard [37] in Maestro, which involves structure preprocessing and refinement stages. The former stage involves using Prime to add hydrogen atoms, generate disulfide bonds and complete missing side-chains. The structure refinement stage comprises removing water molecules, optimizing the hydrogen bonding network by rotating hydroxyl (and thiol) group orientations, producing appropriate tautomeric states of His residues and conducting chi flips of Asn,

Gln and His residues. Finally, a restrained minimization is performed to relax the structure by relieving any strain and modifying heavy atom and hydrogen atom positions.

The series of C9 analogues was docked into the pre-prepared D3 receptor binding pocket using Glide in 'Standard Precision' (SP) mode [38]. This process involved initially generating a receptor grid using an automated protocol in Maestro in which default settings were utilized for the grid parameters. A 10 Å cubic box was specified around the D3 receptor co-crystallized ligand and the analogue compounds were docked within the box. The docking procedure comprised the generation of ligand conformations, which are assessed in terms of the 'fit' of the ligand to the binding cavity and the complementarity of the protein-ligand interactions. This process allows poor scoring poses to be filtered out and those that successfully pass the screening are subsequently minimized using the OPLS_2005 force field [39]. For each C9 analogue, several poses pass the screening process and are minimized. In the final step, these minimized poses are rescored and ranked according to the Glidescore scoring function, which gives an estimate of the binding affinity. The Glidescore of the highest ranked pose for each ligand is shown in Table 2. Overall, the non-brominated C9 analogues were found to have slightly lower Glidescore binding affinity values than the corresponding brominated ligands in agreement with the affinity measurements for these systems.

The non-brominated analogue **22g** showed the highest D3 receptor affinity and to provide further insight into the key interactions in the complex, a representation of the binding pose for **22g** and the corresponding brominated analogue **20g** within the D3 receptor binding cavity are shown in Fig. 2. The structures depicted represent the top-ranked binding modes for each ligand according to Glidescore. The poses for both ligands illustrate the important receptor-ligand interactions for these systems, including the critical quaternary N − Asp110 salt bridge motif, H-bonds to Ser192 and Cys181 and hydrophobic interactions to Phe106 and Phe345 (Fig. 2a). Furthermore, the non-brominated analogue makes an H-bond to Thr369 via the methoxyethyl substituent, whereas the bromine atom of the brominated system makes an additional interaction with the backbone of Ile183. The aromatic groups of the ligands project into the hydrophobic regions of the receptor binding site as illustrated in Fig. 2b. The Glidescore estimates of the binding energy for the two compounds are very similar, −8.0 and −7.8 kcal/mol for **22g** and **20g**, respectively. Overall, the non-brominated ligand **22g** is calculated to have a slightly higher lipophilic interaction energy, whereas the brominated compound **20g** has a slightly better H-bonding energy. Qualitatively, these results match the experimentally observed affinities, however, at the quantitative level, the Glidescore values are too close to clearly differentiate the compounds.

Table 2
Predicted binding affinity from Glidescore for C9 analogues at the D3 receptor.

Compound	R^1	R^2	D3 K_i (nM), GlideScore
20a	Et	Br	373, −7.6
20b	*n*-Pr	Br	195, −7.3
20c	*n*-Bu	Br	>10, 000, −7.1
20d	*n*-Pen	Br	3605, −7.4
20e	*n*-Hex	Br	3171, −7.3
20f	*sec*-Bu	Br	2070, −7.7
20g	Methoxyethyl	Br	726, −7.8
22a	Et	H	106, −7.9
22b	*n*-Pr	H	175, −8.0
22c	*n*-Bu	H	131, −8.1
22d	*n*-Pen	H	3213, −8.0
22e	*n*-Hex	H	195, −8.1
22f	*Sec*-Bu	H	450, −7.8
22g	Methoxyethyl	H	31, −8.0
1	Me	H	30.1, −7.9

The Glidescore outcomes for the C9 alkoxy substituents do not show significant differences as the length of the alkyl chain is increased. For instance, as the C9 alkoxy chain is lengthened from the ethyl to the *n*-hexyl chain (compounds **22a**–**e**), the estimated binding energy changes from −7.9 to −8.1 kcal/mol for the non-brominated ligands. The non-brominated C9 *sec*-butyloxy analogue **22f** also displayed a similar Glidescore energy of −7.8 kcal/mol. These values are all very close to that determined for the lead compound stepholoidine (−7.9 kcal/mol). The experimentally observed affinity values for the non-brominated C9 analogues also showed relatively little variation ranging from 106 to 195 nM with no particular trend as the size of the chain increases, except for the branched *sec*-butyloxy analogue **22f** and the *n*-pentyloxy compound **22d**, which were measured to have significantly lower affinity values of 450 and 3213 nM, respectively. The calculated Glidescore energies did not display these two outliers. In agreement with the experimental data, the corresponding brominated analogues (compounds **20a**–**e**) were found to have lower magnitude Glidescore values from −7.1 to −7.6 kcal/mol with the branched *sec*-butyloxy ligand **20f** having a value of −7.7 kcal/mol. Again, in quantitative terms, there is no discernible trend in binding affinity values as the length of the chain increases or in terms of the chain branching. The *n*-butyloxy analogue **20c** displayed the lowest experimentally observed affinity as well as the lowest Glidescore value, whereas compounds **20d**, **20e** and **20f** with measured affinities greater than 2000 nM had similar Glidescore values to **20a** and **20b**, which had about 10-fold better observed affinities.

The binding poses for the ethoxy and *n*-hexyloxy C9 analogues with and without the bromine substituent within the D3 receptor binding pocket are depicted in Fig. 3. These complexes involve the same key receptor-ligand interactions as discussed above, the quaternary N − Asp110 salt bridge, H-bonds to Ser192 and Cys181 and hydrophobic interactions to Phe106 and Phe345. The brominated analogues make an additional weak halogen bond [32] to the Ile183 backbone, however, this is more than balanced by the higher lipophilic interaction energies of the non-brominated systems. Examination of the D3 receptor binding site shows that the alkoxy groups of the C9 analogues, including the longest *n*-hexyloxy chain, project into the hydrophobic extracellular region of the binding cavity (the secondary binding pocket, SBP), without causing significant clashes with the receptor structure (Fig. 4). The small variation in predicted binding energies according to Glidescore for these systems is, therefore, not surprising, although this does not explain the much larger differences in their measured affinity values. Nevertheless, overall in qualitative terms, the small decrease in the Glidescore binding energy for the brominated compared to the non-brominated compounds is in agreement with the decreased experimental affinity measurements for these ligands.

The behavior of both brominated and non-brominated C9 analogues were analyzed within the D3 binding site through molecular dynamics simulations. Six representative analogues were selected, **20a** (R^1 = Et, R^2 = Br), **20e** (R^1 = *n*-Hex, R^2 = Br), **20g** (R^1 = methoxyethyl, R^2 = Br), **22a** (R^1 = Et, R^2 = H), **22e** (R^1 = *n*-Hex, R^2 = H), and **22g** (R^1 = methoxyethyl, R^2 = H). These six analogues were simulated within the AMBER molecular dynamics program for 100 ns simulation time in isochoric-isothermal conditions. The starting configuration for these six simulations consisted of the docked poses generated above, solvated in 10 Å a box of tip4pew water [42]. Protein atoms were parameterized with Amber14SB [43], ligand parameters were assigned using the general amber force field (gaff) [44]. These configurations were minimized using 20000 steps steepest descent, heated to 300 K over the

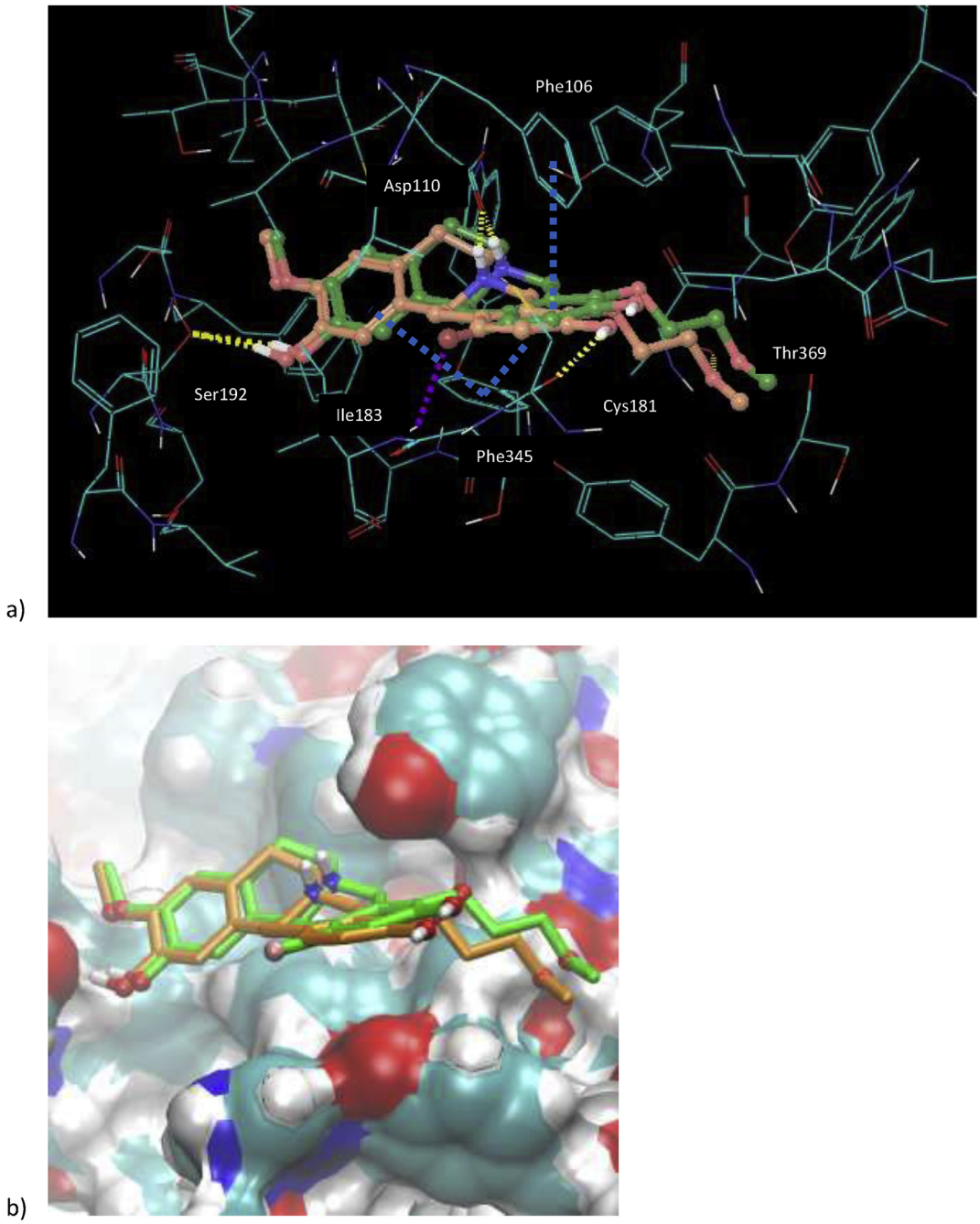

Fig. 2. a) Docked poses of the C9 analogues **20g** (green carbon atoms) and **22g** (brown carbon atoms). Key hydrogen bonding interactions are given by the yellow dashed lines and hydrophobic interactions by the blue dashed lines. The halogen bond [40,41] involving the Br atom is given by the purple dashed line. **b)** Molecular surface of the binding cavity with the docked ligands **20g** and **22g**. The surface is color coded according to the electrostatic potential, with red denoting positive hydrophilic, blue denoting negative hydrophilic, and green representing hydrophobic regions. (For interpretation of the references to colour in this figure legend, the reader is referred to the web version of this article.)

course of 240 ps in isochoric-isothermal conditions, and equilibrated for 20 ns in isobaric-isothermal conditions. During the production simulation protein heavy atoms were restrained with restraint weights of 2.5 kcal/Å^2. The SHAKE algorithm was utilized to maintain hydrogen bond distances, Berendsen barostat to maintain constant pressure, and Langevin thermostat to maintain constant temperatures.

To assess the stability of these six analogues we evaluated two metrics: ligand root mean square deviation compared to their docked poses and ligand distance to the key aspartate (residue 110) throughout the 100 ns production simulation. These six analogues displayed low RMSD's that did not fluctuate significantly over our production simulation (Fig. 5). The highest RMSD found between all six ligands was 1.9 Å by **22e**, an *n*-hexyloxy analogue. The distance between each analogue center of mass and Asp 110 was evaluated to determine whether this key salt bridge contact is maintained. All six analogues displayed extremely stable distances to Asp 110 (Fig. 6). These quantities indicate that during this 100 ns simulation no ligands left the pocket, all ligands maintained the key aspartate salt bridge, and remained similar to the starting docked pose.

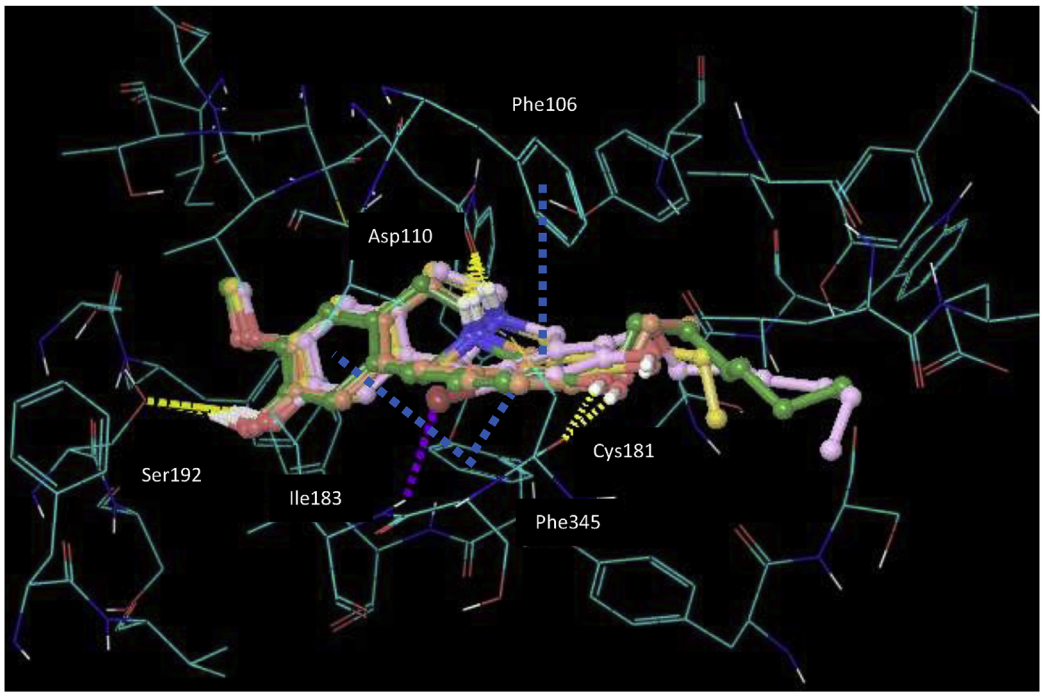

Fig. 3. Docked poses of the brominated C9 analogue molecules **20a** (yellow carbon atoms) and **20e** (pink carbon atoms) and the corresponding non-brominated analogues **22a** (brown carbon atoms) and **22e** (green carbon atoms). Key hydrogen bonding interactions are given by the yellow dashed lines and hydrophobic interactions by the blue dashed lines. The halogen bond involving the Br atom is given by the purple dashed line. (For interpretation of the references to colour in this figure legend, the reader is referred to the web version of this article.)

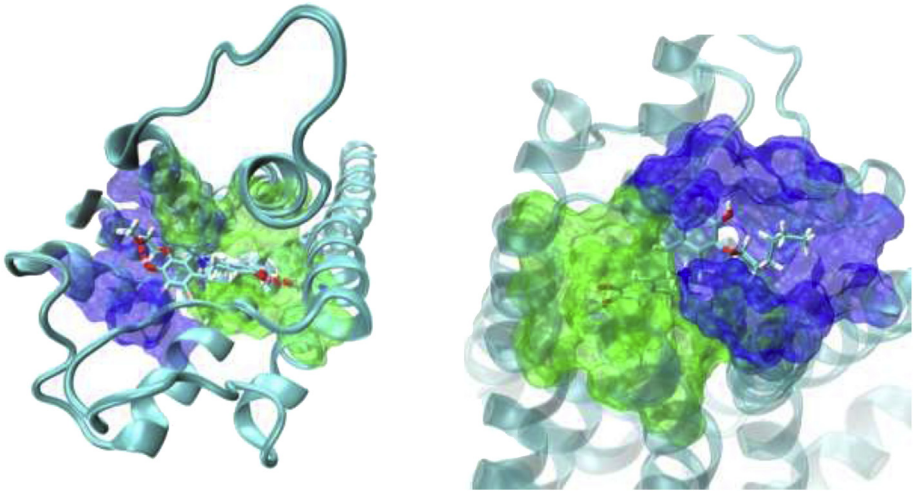

Fig. 4. Ligands **20g** (left) and **22g** (right) bound to D3 (cartoon), orthosteric binding site shown in green and secondary binding pocket (SBP) highlighted in blue. (For interpretation of the references to colour in this figure legend, the reader is referred to the web version of this article.)

3. Conclusions

This is the first study that investigates the effects of alkoxy substitutions at the C9 position (alone or in tandem with C12 bromination) of (-)-stepholidine on affinity at D1, D2 and D3 receptors. In general, C9 alkoxy substituents impart D1 selectivity to the scaffold. C12 bromination has opposite effects on D1 and D3 affinities – C12 bromination tends to increase D1 affinity (particularly for small substituent groups) but reduces D3 affinity. C9 alkoxylation reduces D3 affinity, except in the case of compound **22g**. Some C9 alkoxy compounds lacked affinity for the D2 receptor but it is still not clear how steric or electronic factors account for the lack of D2 receptor affinity. Compound **22a** was found to be a dual D1/D3 receptor antagonist – thus it appears that extension of the C9 alkoxy chain of (-)-stepholidine reverses D1 functional activity.

In comparison to the experimentally measured ligand affinities, the Glidescore estimated binding energies from the D3 receptor docking simulations show some similarities and differences. This is perhaps unsurprising, as empirical scoring functions, such as Glidescore used in this work, typically work well in qualitatively distinguishing active from inactive ligands, however, they are often less successful at quantitatively rank ordering docked poses according to the scoring function values. Further aspects of the current work that probably prevented a definitive association between

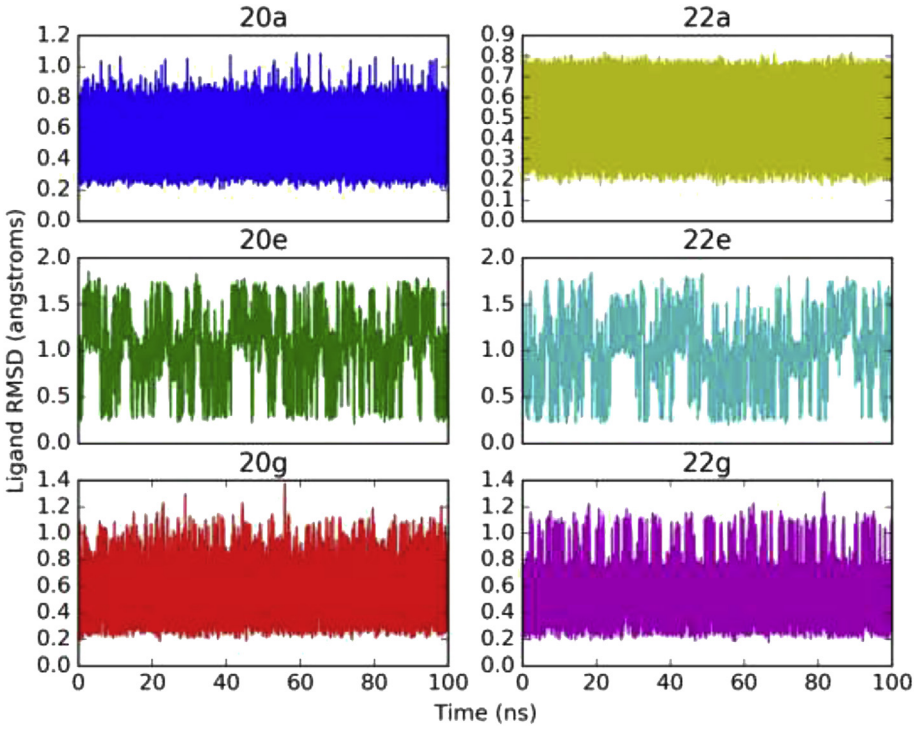

Fig. 5. Root mean square deviation computed for six (-)-stepholidine analogues (**22a**, **22e**, **22g**, **20a**, **20e**, **20g**) over the course of a 100 ns simulation. RMSD was calculated at every 1 ps to the reference position of the ligands in the docked configuration. All six ligands display stability within the pocket during the sampled time, with the highest achieved RMSD of 1.9 Å.

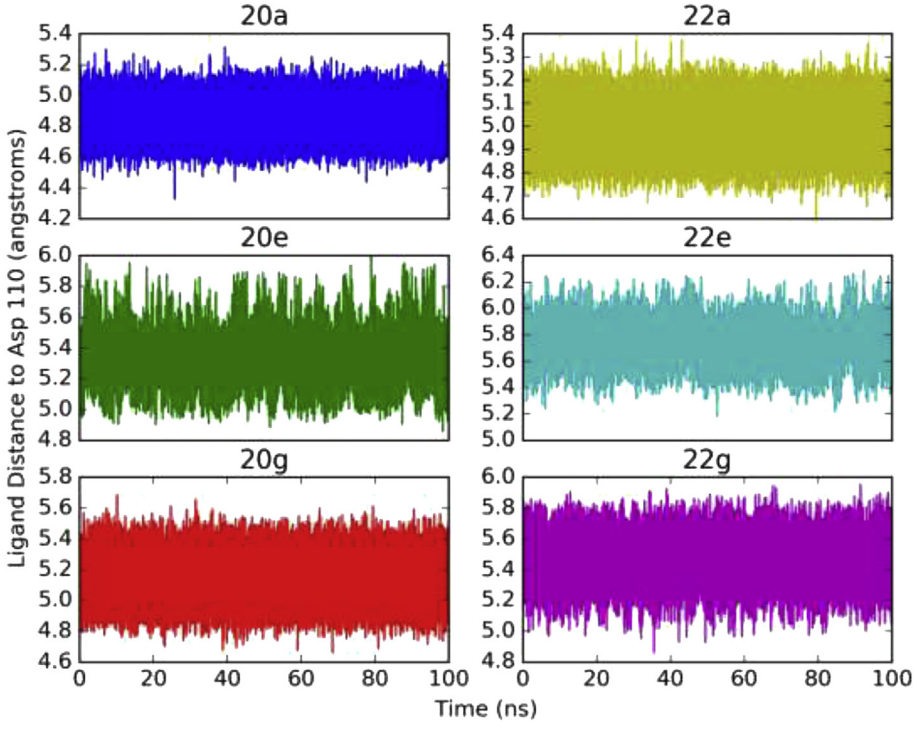

Fig. 6. Ligand distance of six (-)-stepholidine analogues (**20a**, **20e**, **20g**, **22a**, **22e**, **22g**) over the course of a 100 ns simulation. This distance was computed every 1 ps between the ligand center of mass and residue 110, a key conserved aspartate contact. All six ligands display minor fluctuations in their position relative to this contact throughout the sampled time, strongly implying each remains bound.

the docking scores and experimentally measured affinities include the small number of ligands studied in the biological assays and the docking simulations, the small observed affinity range for some of the ligands and the generation of multiple binding modes for each ligand in the receptor binding cavity. More extended studies comprising a larger and more diverse series of ligands would be

needed to afford deeper insight and quantitative assessment of the performance of our ligand docking process. Nevertheless, despite these features, the *in silico* docking model was capable of successfully distinguishing between the brominated and non-brominated C9 analogues and allowed for the recognition of key protein-ligand interactions within the D3 receptor binding pocket that need to be retained in the exploration of diverse and selective ligands with high affinity.

Modifications at C9 may be a means to generate dual potent selective D1/D3 ligands, but will be challenging especially with regards to obtaining high D3 receptor affinity. Further SAR and computational work on the scaffold is necessary to fulfill this goal. In order to provide deeper insight into the ligand requirements for D1/D3 selectivity, we have initiated docking studies into binding pockets of D1 and D2 receptor structures derived from homology models in comparison to D3. This is a large scale project that will form the central theme of a future publication. Our work demonstrates that a C-9 alkoxy, C10-hydroxy substitution pattern in ring D delivers selective D1 ligands and has uncovered novel and unique D1/D3 selective ligands that are useful leads for further optimization.

4. Experimental

General experimental procedures: All moisture-sensitive and oxygen-sensitive reactions were carried out in flame-dried glassware under a nitrogen atmosphere. Solvents and all other reagents were purchased at the highest commercial quality from Aldrich and Fisher Scientific USA and used without further purification. Anhydrous sodium sulfate was used as drying agent for work-up of reactions. HRESIMS spectra were obtained using an Agilent 6520 QTOF instrument. ^{1}H NMR and ^{13}C NMR spectra were recorded using or Bruker DPX-600 spectrometer (operating at 600 MHz for ^{1}H; 150 MHz, for ^{13}C) or Bruker DPX-500 spectrometer (operating at 500 MHz for ^{1}H; 125 MHz, for ^{13}C) or Bruker DPX-400 spectrometer (operating at 400 MHz for ^{1}H; 100 MHz, for ^{13}C) using $CDCl_3$ as solvent, unless stated otherwise. Tetramethylsilane (0.00 ppm) served as an internal standard in ^{1}H NMR and $CDCl_3$, 77.0 ppm) in ^{13}C NMR unless stated otherwise. Chemical shift (0.00 ppm) values are reported in parts per million and coupling constants in Hertz (Hz). Splitting patterns are described as singlet (s), doublet (d), triplet (t), and multiplet (m). Reactions were monitored by TLC with Whatman Flexible TLC silica gel G/UV 254 precoated plates (0.25 mm). TLC plates were visualized by UV (254 nm) and by staining in an iodine chamber. Flash column chromatography was performed with silica gel 60 (EMD Chemicals, 230–400 mesh, 0.063 mm particle size).

4-benzyloxy-3-hydroxybenzaldehyde (7): To a stirring solution of 3,4-dihydroxybenzaldehyde, **6** (25.0 g, 181.0 mmol) in anhydrous acetonitrile (300 mL), was added K_2CO_3 (25.0 g, 181.0 mmol) followed by benzyl bromide (34.4 mL, 289.6 mmol) slowly, at room temperature, under an inert (N_2) atmosphere. The resulting reaction was heated to reflux and stirring was continued for 2 h. The reaction solvent was removed by evaporation under reduced pressure and to the resulting residue was added cold 10% NaOH solution and stirred for 10 min, after which ethyl acetate (100 mL) was added. The resulting biphasic mixture was separated and the aqueous layer was acidified with 4 N HCl and extracted with DCM (3 × 300 mL). The combined organic layer was washed with brine solution, water, dried over Na_2SO_4, and concentrated under reduced pressure to obtain a residue, which was purified by crystallization using ethyl acetate to afford **7** (31.0 g, 75%). ^{1}H NMR (400 MHz, $CDCl_3$): δ 9.83 (s, 1H, CHO), 7.46–7.38 (m, 7H, ArH), 7.03 (d, J = 8.2 Hz, 1H, ArH), 5.81 (s, 1H, OH), 5.20 (s, 2H, OCH_2Ph); ^{13}C NMR (100 MHz, $CDCl_3$): δ 190.9, 150.9, 146.3, 135.2, 130.8, 128.9 × 2, 128.8, 127.9 × 2, 124.3, 114.4, 111.5, 71.2; HRMS (ESI) *m/z* calcd. for $C_{14}H_{12}O_3$ ([M+H]$^+$), 229.0859, found 229.0863.

4-benzyloxy-3-(*tert*-butyldiphenylsilyloxy)benzaldehyde (8): To a stirred solution of compound **7** (30.0 g, 131.43 mmol) in anhydrous DCM (350 mL) was added TEA (21.89 mL, 157.72 mmol), DMAP (0.16 g, 1.31 mmol), and TBDPSCl (37.59 mL, 144.57 mmol) at 0 °C, under N_2. The reaction mixture was allowed to attain room temperature and stirring was continued overnight. The reaction mixture was diluted with DCM (20 mL), washed with brine and water, dried over Na_2SO_4, and concentrated under reduced pressure to obtain a residue (61.0 g, quantitative). The resulting residue, **8** was utilized for the next reaction without any further purification. ^{1}H NMR (600 MHz, $CDCl_3$): δ 9.62 (s, 1H, CHO), 7.68–7.66 (m, 4H, ArH), 7.40–7.27 (m, 10H, ArH), 7.24–7.23 (m, 1H, ArH), 7.19–7.18 (m, 2H, ArH), 6.88 (d, J = 8.3 Hz, 1H, ArH), 4.90 (s, 2H, OCH_2Ph), 1.08 (s, 9H); ^{13}C NMR (150 MHz, $CDCl_3$): δ 190.6, 155.2, 145.6, 135.9, 135.3 × 3, 132.9, 130.0, 129.8 × 2, 128.4, 128.0 × 2, 127.7 × 3, 127.6 × 3, 127.4 × 2, 125.2, 120.3, 112.7, 70.4, 26.5 × 3, 19.7; HRMS (ESI) *m/z* calcd. for $C_{30}H_{30}O_3Si$ ([M+H]$^+$), 467.2037, found 467.2039.

4-benzyloxy-2-bromo-5-(*tert*-butyldiphenylsilyloxy)benzaldehyde (9): To a stirred solution of compound **8** (20.0 g, 42.85 mmol) in methanol (300 mL) was added bromine (2.19 mL, 42.85 mmol) slowly, at 0 °C, under N_2. The reaction mixture was allowed to attain room temperature and stirring was continued for 2 h. The solvent was removed by evaporation under reduced pressure and the resulting residue was dissolved in ethyl acetate (250 mL) and washed consecutively with brine solution and water. The organic layer was dried over Na_2SO_4, and concentrated under reduced pressure to obtain a residue, which was purified by column chromatography on silica gel using 10:90 and 12:88, EtOAC:Hexanes as eluent to afford compound **9** (20.0 g, 85%). ^{1}H NMR (600 MHz, $CDCl_3$): δ 10.01 (s, 1H, CHO), 7.63–7.62 (m, 4H, ArH), 7.40–7.38 (m, 2H, ArH), 7.31–7.28 (m, 8H, ArH), 7.18–7.16 (m, 2H, ArH), 6.99 (s, 1H, ArH), 4.87 (s, 2H, OCH_2Ph), 1.06 (s, 9H, C$(CH_3)_3$); ^{13}C NMR (150 MHz, $CDCl_3$): δ 190.4, 155.3, 145.0, 135.3 × 3, 135.2 × 3, 132.6, 129.9 × 2, 128.5 × 2, 128.2 × 2, 127.7 × 3, 127.6 × 2, 126.6, 120.2, 119.9, 117.2, 70.8, 26.5 × 3, 19.7; HRMS (ESI) *m/z* calcd. for $C_{30}H_{29}BrNO_3Si$ ([M+H]$^+$), 545.1142, found 545.1146.

[4-benzyloxy-2-bromo-5-(*tert*-butyldiphenylsilyloxy)]phenylmethanol (10): To a stirred solution of compound **9** (20 g, 36.66 mmol) in methanol (200 mL) was added $NaBH_4$ (1.66 g, 43.99 mmol) in portion wise, at 0 °C, under N_2. The reaction mixture was allowed to come to room temperature and stirring was continued for 1 h. Thereafter the reaction was quenched with methanol. The solvent was removed by evaporation under reduced pressure and the resulting residue was dissolved in ethyl acetate (250 mL) and washed consecutively with brine and water. The organic layer was dried over Na_2SO_4, and concentrated under reduced pressure to obtain a residue, which was purified by column chromatography on silica gel using 20:80 EtOAC:Hexanes as eluent to afford compound **10** (18.7 g, 93%). ^{1}H NMR (600 MHz, $CDCl_3$): δ 7.67–7.65 (m, 4H, ArH), 7.38–7.35 (m, 2H, ArH), 7.30–7.25 (m, 7H, ArH), 7.20–7.19 (m, 2H, ArH), 6.98 (s, 1H, ArH), 6.78 (s, 1H, ArH), 4.82 (s, 2H, OCH_2Ph), 4.37 (d, J = 4.8 Hz, 2H, CH_2OH), 1.07 (s, 9H, C$(CH_3)_3$); ^{13}C NMR (150 MHz, $CDCl_3$): δ 149.6, 144.8, 136.3, 135.3 × 3, 133.1, 132.1, 129.7 × 2, 128.3 × 3, 127.8 × 2, 127.6 × 3, 127.4 × 3, 120.8, 117.8, 113.2, 70.8, 64.5, 26.5 × 3, 19.6; HRMS (ESI) *m/z* calcd. for $C_{30}H_{31}BrO_3Si$ ([M+Na]$^+$), 569.1103, found 569.1102.

[2-benzyloxy-4-bromo-5-(bromomethyl)]phenoxy-*tert*-butyldiphenylsilane (11): To a stirred solution of compound **10** (18.5 g, 33.78 mmol) in anhydrous DCM (200 mL) was added phosphorous tribromide (1.74 mL, 18.58 mmol) slowly, at 0 °C, under N_2. The reaction mixture was allowed to stir at room temperature for 2 h. Then the reaction mixture was quenched with aqueous $NaHCO_3$ solution. The organic layer was separated and

washed consecutively with brine solution and water. The organic layer was dried over Na_2SO_4, and concentrated under reduced pressure to obtain a residue, which was purified by column chromatography on silica gel using 12:88, EtOAC:Hexanes as eluent to afford compound, **9** (17.0 g, 82%). ^{1}H NMR (600 MHz, $CDCl_3$): δ 7.66–7.64 (m, 4H, ArH), 7.40–7.38 (m, 2H, ArH), 7.32–7.27 (m, 7H, ArH), 7.22–7.20 (m, 2H, ArH), 6.98 (s, 1H, ArH), 6.74 (s, 1H, ArH), 4.84 (s, 2H, OC*H*$_2$Ph), 4.30 (s, 2H, CH_2Br), 1.06 (s, 9H, C(CH_3)$_3$); ^{13}C NMR (150 MHz, $CDCl_3$): δ 150.6, 144.7, 136.0, 135.3 × 3, 132.8, 129.8 × 2, 128.9 × 3, 128.4, 127.9 × 3, 127.6 × 3, 127.4 × 2, 122.4, 117.8, 115.2, 70.8, 33.7, 26.5 × 3, 19.7; HRMS (ESI) *m/z* calcd. for $C_{30}H_{30}Br_2O_2Si$ ([M+H]$^+$), 600.1744, found 600.1751.

2-(4-(benzyloxy)-2-bromo-5-[(*tert*-butyldiphenylsilyloxy) phenyl]acetonitrile (12): To a stirred solution of compound **11** (17.0 g, 27.84 mmol) in anhydrous DMF (150 mL) was added NaCN (2.73 g, 55.69 mmol), at room temperature, under N_2 and stirring was continued for 2 h. Then reaction mixture was cooled to 0 °C, quenched with aqueous hypochlorite solution and stirring was continued for 15 min. The solvent was removed by evaporation under reduced pressure and the resulting residue was dissolved in ethyl acetate (200 mL) and washed with brine solution and water. The organic layer was dried over Na_2SO_4, and concentrated under reduced pressure to obtain a residue, which was purified by column chromatography on silica gel using 70:30 and 80:20 (gradient elution), EtOAC:Hexanes as eluent to afford compound, **12** (12.6 g, 81%). ^{1}H NMR (600 MHz, $CDCl_3$): δ 7.66–7.65 (m, 4H, ArH), 7.42–7.39 (m, 2H, ArH), 7.33–7.28 (m, 7H, ArH), 7.21–7.20 (m, 2H, ArH), 7.00 (s, 1H, ArH), 6.78 (s, 1H, ArH), 4.84 (s, 2H, OC*H*$_2$Ph), 3.50 (s, 2H, CH_2CN), 1.06 (s, 9H, C(CH_3)$_3$); ^{13}C NMR (150 MHz, $CDCl_3$): δ 150.2, 145.2, 136.0, 135.3 × 3, 132.7 × 2, 129.9 × 2, 128.4 × 2, 127.9 × 2, 127.7 × 3, 127.4 × 2, 121.7, 121.2 × 2, 117.9, 116.8, 114.1, 70.9, 26.5 × 3, 23.9, 19.7; HRMS (ESI) *m/z* calcd. for $C_{31}H_{30}BrNO_2Si$ ([M+Na]$^+$), 578.1121, found 578.1124.

2-(4-(benzyloxy)-2-bromo-5-hydroxyphenyl)acetic acid (13): To a stirred solution of compound, **12** (12.5 g, 22.45 mmol) in a mixture of ethanol (65 mL) and water (65 mL) was added NaOH (2.69 g, 67.37 mmol), at room temperature. The resulting reaction mixture was heated at 75 °C for 3 h, then another portion of NaOH (1.79 g, 44.91 mmol) was added to the reaction mixture and stirring was continued for another 2 h. The solvent was removed by evaporation under reduced pressure and the resulting residue was dissolved in water (150 mL) and washed with ethyl acetate. The aqueous layer was cooled to 0 °C, and acidified (pH ~2) with 3 N HCl. During the acidification product was precipitated out, which was filtered and dried under vacuum to afford **13** (6.14 g, 81%). ^{1}H NMR (600 MHz, $CDCl_3$): δ 7.43–7.36 (m, 5H, ArH), 7.12 (s, 1H, ArH), 6.90 (s, 1H, ArH), 5.07 (s, 2H, OC*H*$_2$Ph), 3.73 (s, 2H, C*H*$_2$COOH); ^{13}C NMR (150 MHz, $CDCl_3$): δ 176.2, 145.8, 145.3, 135.5, 128.9, 128.8, 128.7, 128.0, 127.9, 126.5, 117.3, 116.3, 113.9, 71.5, 40.6; HRMS (ESI) *m/z* calcd. for $C_{15}H_{14}BrO$ ([M+H]$^+$), 337.0075, found 337.0068.

2-(4-(benzyloxy)-2-bromo-5-hydroxyphenyl)-N-(4-(benzyloxy)-3-methoxyphenethyl)acetamide (15): To a mixture of **13** (5.0 g, 14.88 mmol), and amine **14** (3.82 g, 14.88 mmol) in anhydrous DMF (75 mL) was added EDCI (3.12 g, 16.36 mmol) followed by TEA (1.86 mL, 13.39 mmol), at 0 °C. The resulting reaction mixture was warmed to room temperature and stirring was continued for overnight. The solvent was removed by evaporation under reduced pressure and the resulting residue was dissolved in ethyl acetate (100 mL) and washed with brine solution and water. The organic layer was dried over Na_2SO_4, and concentrated under reduced pressure to obtain a residue, which was purified by column chromatography on silica gel using 2:98 MeOH:DCM as eluent to afford compound, **15** (3.80 g, 43%). ^{1}H NMR (400 MHz, $CDCl_3$): δ 7.42–7.27 (m, 10H, ArH), 7.05 (s, 1H, ArH), 6.85 (s, 1H, ArH), 6.76 (d, *J* = 8.1 Hz, 1H, ArH), 6.64 (d, *J* = 1.8 Hz, 1H, ArH), 6.54 (dd, *J* = 8.1, 1.9 Hz, 1H, ArH), 5.69 (brs, 1H, OH), 5.40–5.37 (m, 1H, NH), 5.10 (s, 2H, OC*H*$_2$Ph), 5.05 (s, 2H, OC*H*$_2$Ph), 3.83 (s, 3H, OCH_3), 3.54 (s, 2H, CH_2), 3.47–3.42 (m, 2H, CH_2C*H*$_2$N), 2.68 (t, *J* = 6.8 Hz, 2H, C*H*$_2$$CH_2$N); ^{13}C NMR (100 MHz, $CDCl_3$): δ 169.6, 149.7, 146.8, 145.8, 145.5, 137.2, 135.4, 131.8 × 2, 128.8, 128.7, 128.6, 128.5, 128.0 × 2, 127.7, 127.6, 127.5, 127.2 × 2, 120.6, 117.3, 116.4, 113.7, 112.4, 71.5, 71.2, 55.9, 43.5, 40.7, 35.0; HRMS (ESI) *m/z* calcd. for $C_{31}H_{30}BrNO_5$ ([M+H]$^+$), 576.1380, found 576.1377.

2-(benzyloxy)-5-[(7-(benzyloxy)-6-methoxy-3,4-dihydroisoquinolin-1-yl)methyl]-4-bromophenol (16): To a stirred solution of compound, **15** (3.75 g, 6.52 mmol) in anhydrous acetonitrile (40 mL) was added $POCl_3$ (3.0 mL, 32.60 mmol), at room temperature, under N_2. The resulting reaction was heated at 80 °C for 2 h. Then solvent was removed by evaporation under reduced pressure and the resulting residue was quenched with cold saturated $NaHCO_3$ solution and extracted with ethyl acetate (3 × 100 mL). The combined organic layer was washed with brine solution and water, dried over Na_2SO_4, and concentrated to obtain a residue, **16** (crude 3.60 g) which was utilized for the next step without further purification.

(*S*)-2-(benzyloxy)-5-[(7-(benzyloxy)-6-methoxy-1,2,3,4-tetrahydroisoquinolin-1-yl)methyl]-4-bromophenol (17): The imine **16** (3.60 g, 6.46 mmol) was dissolved in anhydrous DMF (20 mL), and the solution purged with nitrogen for 10 min. Then RuCl[(*R,R*)-TsDPEN(P-cymene)] (41.0 mg, 0.06 mmol) was added and purging was continued for a further 5 min. Thereafter a mixture of formic acid (1.36 mL, 36.19 mmol) and triethylamine (0.53 mL, 3.87 mmol) (v/v = 5/2) was added and the reaction mixture was stirred at room temperature overnight. The reaction mixture was adjusted to pH 8 with saturated $NaHCO_3$ and extracted with ethyl acetate. The combined organic layer was washed with brine, dried over Na_2SO_4, and concentrated. The crude product was purified by column chromatography on silica gel using 3:97 to 5:95 MeOH:DCM as eluent to afford compound **17** (1.45 g, 40% over two steps). ^{1}H NMR (500 MHz, $CDCl_3$): δ 7.45–7.43 (m, 2H, ArH), 7.39–7.34 (m, 7H, ArH), 7.29–7.28 (m, 1H, ArH), 7.09 (s, 1H, ArH), 6.83 (s, 1H, ArH), 6.77 (s, 1H, ArH), 6.59 (s, 1H, ArH), 5.12 (s, 2H, OC*H*$_2$Ph), 5.03 (s, 2H, OC*H*$_2$Ph), 4.07 (d, *J* = 7.9 Hz, 1H), 3.87 (s, 3H, OCH_3), 3.21–3.16 (m, 1H), 3.05 (dd, *J* = 13.9, 2.8 Hz, 1H), 2.92–2.87 (m, 1H), 2.78–2.69 (m, 3H); ^{13}C NMR (125 MHz, $CDCl_3$): δ 148.2, 146.1, 145.3, 145.1, 137.4, 135.7, 131.8, 130.5, 128.7 × 2, 128.6, 128.5 × 2, 128.0 × 2, 127.7 × 2, 127.3 × 2, 117.8, 116.4, 113.3, 112.9, 112.1, 71.4, 71.3, 56.0, 54.9, 42.2, 39.7, 29.4; HRMS (ESI) *m/z* calcd. for $C_{31}H_{30}BrNO_4$ ([M+H]$^+$), 560.1436, found 560.1437.

(*S*)-2,10-bis(benzyloxy)-12-bromo-3-methoxy-5,8,13,13a-tetrahydro-6*H*-isoquinolino[3,2-*a*]isoquinolin-9-ol (18): To a stirred solution of compound **17** (1.0 g, 1.78 mmol) in anhydrous methanol (8.0 mL) was added formalin (7.0 mL), at room temperature. The resulting reaction mixture was heated at reflux temperature for 4 h. Then solvent was removed by evaporation under reduced pressure and the resulting residue was dissolved in ethyl acetate (50 mL) and washed with brine solution and water. The organic layer was dried over Na_2SO_4, and concentrated under reduced pressure to obtain a residue, which was purified by column chromatography on silica gel using 2:98 MeOH:DCM as eluent to afford compound, **18** (0.64 g, 63%). ^{1}H NMR (500 MHz, $CDCl_3$): δ 7.47–7.46 (m, 2H, ArH), 7.40–7.35 (m, 7H, ArH), 7.30–7.27 (m, 1H, ArH), 7.03 (s, 1H, ArH), 6.79 (s, 1H, ArH), 6.63 (s, 1H, ArH), 5.71 (brs, 1H, OH), 5.19–5.13 (m, 2H, OC*H*$_2$Ph), 5.06–5.02 (m, 2H, OC*H*$_2$Ph), 4.18 (d, *J* = 15.7 Hz, 1H), 3.87 (s, 3H, OCH_3), 3.46–3.40 (m, 2H), 3.18–3.07 (m, 3H), 2.67–2.47 (m, 3H); ^{13}C NMR (125 MHz, $CDCl_3$): δ 148.3, 146.4, 143.7, 141.2, 137.3, 135.9, 129.4, 128.7 × 2, 128.6, 128.5 × 2, 127.9 × 2, 127.8 × 2, 127.7, 127.4 × 2, 123.4, 114.2, 113.3, 112.2, 111.8, 71.6, 71.5, 59.0, 55.9, 53.5, 51.0, 37.2, 29.0; HRMS (ESI) *m/z* calcd. for $C_{32}H_{30}BrNO_4$ ([M+H]$^+$), 572.1436, found 572.1470.

General synthetic procedure for the compounds 19a-19g as demonstrated for 19a: Compound, **18** (1.0 eq) was dissolved in anhydrous DMF, cooled to 0 °C and K_2CO_3 (2.0 eq) was added, followed by ethyl bromide (1.2 eq). The resulting reaction was allowed to reach ambient temperature and stirring was continued for 2–5 h. The reaction was quenched with cold water and extracted with ethyl acetate (3 × 100 mL). The combined organic layer was washed with brine solution and water, dried over Na_2SO_4, and concentrated to obtain a residue which was purified by column chromatography on silica gel using 25:75 to 50:50 EtOAC:Hexanes as eluent to afford compound **19a** as light yellow sticky solid.

((*S*)-2,10-bis(benzyloxy)-12-bromo-9-ethoxy-3-methoxy-5,8,13,13a-tetrahydro-6*H*-isoquinolino[3,2-*a*]isoquinoline) (19a): Yield: 76% (160 mg from 200 mg); $R_f = 0.60$ on silica gel TLC plate in 25:75/EtOAc: Hexanes; ^{1}H NMR (500 MHz, $CDCl_3$): δ 7.46 (d, *J* = 7.3 Hz, 2H, ArH), 7.42–7.28 (m, 8H, ArH), 7.08 (s, 1H, ArH), 6.79 (s, 1H, ArH), 6.63 (s, 1H, ArH), 5.19–5.13 (m, 2H, OC*H*$_2$Ph), 5.07–5.02 (m, 2H, OC*H*$_2$Ph), 4.21 (d, *J* = 15.8 Hz, 1H), 4.15–4.01 (m, 2H), 3.87 (s, 3H), 3.48–3.42 (m, 2H), 3.19–3.07 (m, 3H), 2.67 (d, *J* = 16.0 Hz, 1H), 2.62–2.57 (m, 1H), 2.53–2.47 (m, 1H), 1.34 (t, *J* = 7.1 Hz, 3H); ^{13}C NMR (125 MHz, $CDCl_3$): δ 149.8, 148.3, 146.4, 144.2, 137.3, 136.6, 130.9, 129.3, 128.6 × 2, 128.5 × 2, 128.0, 127.8, 127.6, 127.5 × 2, 127.4 × 2, 127.3, 118.0, 116.6, 112.2, 111.8, 71.6, 71.1, 68.5, 59.0, 55.9, 54.3, 51.1, 37.3, 29.0, 15.8; HRMS (ESI) *m/z* calcd. for $C_{34}H_{34}BrNO_4$ ($[M+H]^+$), 600.1744, found 600.1751.

((*S*)-2,10-bis(benzyloxy)-12-bromo-3-methoxy-9-propoxy-5,8,13,13a-tetrahydro-6H-isoquinolino[3,2-*a*]isoquinoline) (19b): Yield: 72% (154 mg from 200 mg), light yellow gum; $R_f = 0.60$ on silica gel TLC plate in 25:75/EtOAc: Hexanes; ^{1}H NMR (500 MHz, $CDCl_3$): δ 7.46 (d, *J* = 7.3 Hz, 2H, ArH), 7.42–7.28 (m, 8H, ArH), 7.08 (s, 1H, ArH), 6.79 (s, 1H, ArH), 6.63 (s, 1H, ArH), 5.19–5.13 (m, 2H, OC*H*$_2$Ph), 5.07–5.01 (m, 2H, OC*H*$_2$Ph), 4.21 (d, *J* = 15.8 Hz, 1H), 4.02–3.97 (m, 1H), 3.94–3.88 (m, 1H), 3.87 (s, 3H), 3.49–3.42 (m, 2H), 3.19–3.07 (m, 3H), 2.67 (d, *J* = 16.0 Hz, 1H), 2.62–2.57 (m, 1H), 2.53–2.47 (m, 1H), 1.78–1.71 (m, 2H), 0.98 (t, *J* = 7.4 Hz, 3H); ^{13}C NMR (125 MHz, $CDCl_3$): δ 149.8, 148.3, 146.5, 144.3, 137.3, 136.6, 130.8, 129.4, 128.6 × 2, 128.5 × 2, 128.0, 127.8 × 2, 127.6, 127.5 × 2, 127.4 × 2, 117.9, 116.6, 112.2, 111.8, 74.4, 71.6, 71.1, 59.0, 55.9, 54.2, 51.1, 37.3, 29.0, 23.6, 10.5; HRMS (ESI) *m/z* calcd. for $C_{35}H_{36}BrNO_4$ ($[M+H]^+$), 614.1900, found 614.1900.

((*S*)-2,10-bis(benzyloxy)-12-bromo-9-butoxy-3-methoxy-5,8,13,13a-tetrahydro-6H-isoquinolino[3,2-*a*]isoquinoline) (19c): Yield: 70% (115 mg from 150 mg), light yellow gum; $R_f = 0.63$ on silica gel TLC plate in 25:75/EtOAc: Hexanes; ^{1}H NMR (500 MHz, $CDCl_3$): δ 7.47–7.29 (m, 10H, ArH), 7.08 (s, 1H, ArH), 6.79 (s, 1H, ArH), 6.63 (s, 1H, ArH), 5.17 (d, *J* = 3.6 Hz, 2H, OC*H*$_2$Ph), 5.05 (d, *J* = 2.1 Hz, 2H, OC*H*$_2$Ph), 4.20 (d, *J* = 15.8 Hz, 1H), 4.06–4.01 (m, 1H), 3.97–3.93 (m, 1H), 3.88 (s, 3H), 3.49–3.42 (m, 2H), 3.19–3.07 (m, 3H), 2.67 (d, *J* = 16.0 Hz, 1H), 2.63–2.57 (m, 1H), 2.53–2.47 (m, 1H), 1.73–1.68 (m, 2H), 1.48–1.40 (m, 2H), 0.91 (t, *J* = 7.3 Hz, 3H); ^{13}C NMR (500 MHz, $CDCl_3$): δ 149.8, 148.3, 146.5, 144.3, 137.3, 136.6, 130.8, 129.4, 128.6 × 2, 128.5 × 2, 128.0, 127.8 × 2, 127.6, 127.5 × 2, 127.4 × 2, 117.9, 116.6, 112.2, 111.8, 72.6, 71.6, 71.1, 59.0, 56.0, 54.2, 51.1, 37.3, 32.4, 29.0, 19.2, 13.8; HRMS (ESI) *m/z* calcd. for $C_{36}H_{38}BrNO_4$ ($[M+H]^+$), 628.2057, found 628.2057.

((*S*)-2,10-bis(benzyloxy)-12-bromo-3-methoxy-9-(pentyloxy)-5,8,13,13a-tetrahydro-6H-isoquinolino[3,2-*a*]isoquinoline) (19d): Yield: 77% (130 mg from 150 mg), light brown gum; $R_f = 0.61$ on silica gel TLC plate in 25:75/EtOAc: Hexanes; ^{1}H NMR (500 MHz, $CDCl_3$): δ δ 7.46 (d, *J* = 7.2 Hz, 2H, ArH), 7.43–7.29 (m, 8H, ArH), 7.08 (s, 1H, ArH), 6.79 (s, 1H, ArH), 6.63 (s, 1H, ArH), 5.19–5.14 (m, 2H, OC*H*$_2$Ph), 5.08–5.04 (m, 2H, OC*H*$_2$Ph), 4.20 (d, *J* = 15.8 Hz, 1H), 4.05–4.00 (m, 1H), 3.96–3.92 (m, 1H), 3.88 (s, 3H), 3.49–3.43 (m, 2H), 3.19–3.08 (m, 3H), 2.67 (d, *J* = 16.0 Hz, 1H), 2.63–2.58 (m, 1H), 2.53–2.47 (m, 1H), 1.75–1.70 (m, 2H), 1.40–1.30 (m, 4H), 0.88 (t, *J* = 7.2 Hz, 3H); ^{13}C NMR (125 MHz, $CDCl_3$): δ 149.8, 148.3, 146.5, 144.3, 137.3, 136.6, 130.8, 129.4, 128.6 × 2, 128.5 × 2, 128.0, 127.8, 127.6, 127.5 × 3, 127.4 × 2, 117.9, 116.6, 112.2, 111.8, 72.9, 71.6, 71.1, 59.0, 56.0, 54.2, 51.1, 37.3, 30.0, 29.0, 28.1, 22.4, 14.0; HRMS (ESI) *m/z* calcd. for $C_{37}H_{40}BrNO_4$ ($[M+H]^+$), 642.2213, found 642.2202.

((*S*)-2,1010-bis(benzyloxy)-12-bromo-9-(hexyloxy)-3-methoxy-5,8,13,13a-tetrahydro-6H-isoquinolino[3,2-*a*]isoquinoline) (19e): Yield: 82% (142 mg from 150 mg), light yellow gum; $R_f = 0.61$ on silica gel TLC plate in 25:75/EtOAc: Hexanes; ^{1}H NMR (500 MHz, $CDCl_3$): δ δ 7.46 (d, *J* = 7.5 Hz, 2H, ArH), 7.42–7.28 (m, 8H, ArH), 7.08 (s, 1H, ArH), 6.79 (s, 1H, ArH), 6.63 (s, 1H, ArH), 5.19–5.13 (m, 2H, OC*H*$_2$Ph), 5.05–5.00 (m, 2H, OC*H*$_2$Ph), 4.20 (d, *J* = 15.8 Hz, 1H), 4.05–4.00 (m, 1H), 3.96–3.92 (m, 1H), 3.88 (s, 3H), 3.49–3.43 (m, 2H), 3.19–3.08 (m, 3H), 2.67 (d, *J* = 16.0 Hz, 1H), 2.63–2.58 (m, 1H), 2.53–2.48 (m, 1H), 1.74–1.69 (m, 2H), 1.43–1.7 (m, 2H), 1.31–1.25 (m, 4H), 0.88 (t, *J* = 6.9 Hz, 3H); ^{13}C NMR (125 MHz, $CDCl_3$): δ 149.8, 148.3, 146.5, 144.3, 137.3, 136.6, 130.8, 129.4, 128.6 × 2, 128.5 × 2, 128.0, 127.8, 127.6, 127.4 × 3, 127.3 × 2, 117.9, 116.6, 112.2, 111.8, 72.9, 71.6, 71.1, 59.0, 55.9, 54.2, 51.1, 37.2, 31.6, 30.3, 29.0, 25.6, 22.6, 14.0; HRMS (ESI) *m/z* calcd. for $C_{38}H_{42}BrNO_4$ ($[M+H]^+$), 656.2370, found 656.2374.

((13a*S*)-2,10-bis(benzyloxy)-12-bromo-9-(*sec*-butoxy)-3-methoxy-5,8,13,13a-tetrahydro-6H-isoquinolino[3,2-*a*]isoquinoline) (19f): Yield: 64% (105 mg from 150 mg), light brown gum; $R_f = 0.62$ on silica gel TLC plate in 25:75/EtOAc: Hexanes; ^{1}H NMR (500 MHz, $CDCl_3$): δ 7.46 (d, *J* = 7.4 Hz, 2H, ArH), 7.47–7.29 (m, 8H, ArH), 7.08 (d, *J* = 2.2 Hz, 1H, ArH), 6.79 (s, 1H, ArH), 6.62 (s, 1H, ArH), 5.19–5.13 (m, 2H, OC*H*$_2$Ph), 5.04–4.98 (m, 2H, OC*H*$_2$Ph), OC*H*$_2$Ph), 4.47–4.23 (m, 1H), 4.20 (dd, *J* = 5.3, 15.8 Hz, 1H), 3.87 (s, 3H), 3.44–3.38 (m, 2H), 3.17–3.07 (m, 3H), 2.67 (d, *J* = 15.9 Hz, 1H), 2.60–2.48 (m, 2H), 1.75–1.68 (m, 1H), 1.57–1.52 (m, 1H), 1.18–1.15 (m, 3H), 0.91–0.86 (m, 3H); ^{13}C NMR (125 MHz, $CDCl_3$): δ 149.8, 148.3, 146.4, 142.9, 142.8, 137.3, 136.5, 131.4, 131.3, 129.5, 129.4, 128.6, 128.5, 128.0, 127.8, 127.6, 127.5, 127.4, 127.3, 117.4, 116.5, 116.5, 112.2, 111.8, 79.0, 71.6, 71.2, 59.0, 55.9, 54.8, 51.1, 37.2, 29.8, 29.0, 19.6, 9.8; HRMS (ESI) *m/z* calcd. for $C_{36}H_{38}BrNO_4$ ($[M+H]^+$), 628.2057, found 628.2046.

((*S*)-2,10-bis(benzyloxy)-12-bromo-3-methoxy-9-(2-methoxyethoxy)-5,8,13,13a-tetrahydro-6H-isoquinolino[3,2-*a*] isoquinoline) (19g): Yield: 76% (151 mg from 180 mg), light brown gum; $R_f = 0.52$ on silica gel TLC plate in 25:75/EtOAc: Hexanes; ^{1}H NMR (400 MHz, $CDCl_3$): δ 7.47–7.26 (m, 10H, ArH), 7.08 (s, 1H, ArH), 6.79 (s, 1H, ArH), 6.62 (s, 1H, ArH), 5.19–5.12 (m, 2H, OC*H*$_2$Ph), 5.06–5.00 (m, 2H, OC*H*$_2$Ph), 4.27 (d, *J* = 16 Hz, 1H), 4.24–4.19 (m, 1H), 4.13–4.08 (m, 1H), 3.86 (s, 3H), 3.63–3.60 (m, 2H), 3.50–3.41 (m, 2H), 3.37 (s, 3H), 3.19–3.05 (m, 3H), 2.68–2.47 (m, 3H); ^{13}C NMR (400 MHz, $CDCl_3$): δ 149.6, 148.3, 146.4, 143.9, 137.3, 136.4, 131.0, 129.4, 128.6 × 2, 128.5 × 2, 128.0, 127.8, 127.6, 127.5 × 3, 127.4 × 2, 118.2, 116.5, 112.2, 111.8, 71.8, 71.7, 71.5, 71.1, 59.0, 58.8, 55.9, 54.0, 51.0, 37.2, 29.0; HRMS (ESI) *m/z* calcd. for $C_{35}H_{36}BrNO_5$ ($[M+H]^+$), 630.1855, found 630.1862.

General synthetic procedure for the compounds 20a–20g as demonstrated for 20a: To a stirred solution of compound **19a** (34 mg) in ethanol (4 mL) was added conc. HCl (1 mL), at room temperature. The resulting reaction mixture was refluxed for 2 h. Then the solvent was removed by evaporation under reduced pressure and the resulting residue was basified using aqueous ammonia solution and extracted with ethyl acetate (10 mL × 2). The combined organic layer was washed with brine solution and water, dried over Na_2SO_4, and concentrated under reduced pressure to obtain a residue, which was purified by column chromatography on silica gel using 2:98 MeOH:DCM as eluent to afford compound **20a** as an off-white amorphous solid.

((*S*)-12-bromo-9-ethoxy-3-methoxy-5,8,13,13a-tetrahydro-6H-isoquinolino[3,2-*a*]isoquinoline-2,10-diol) (20a): Yield: 76%

(34 mg from 60 mg),; R_f = 0.42 on silica gel TLC plate in 40:60/EtOAc: Hexanes; ^{1}H NMR (500 MHz, $CDCl_3$): δ 6.99 (s, 1H, ArH), 6.88 (s, 1H, ArH), 6.60 (s, 1H, ArH), 5.59 (br. s, 1H), 4.22 (d, *J* = 15.1 Hz, 1H), 3.98–3.87 (m, 5H), 3.52 (dd, *J* = 11.3, 4.1 Hz, 1H), 3.44 (d, *J* = 15.1 Hz, 1H), 3.29–3.11 (m, 3H), 2.71–2.57 (m, 3H), 1.39 (t, *J* = 7.0 Hz, 3H); ^{13}C NMR (125 MHz, $CDCl_3$): δ 147.4, 145.2, 144.0, 142.4, 130.0, 129.7, 126.5, 125.6, 119.1, 118.7, 111.4, 110.6, 69.0, 59.4, 55.9, 53.9, 51.3, 37.0, 28.9, 15.8; HRMS (ESI) *m/z* calcd. for $C_{20}H_{22}BrNO_4$ ([M+H]$^+$), 420.0810, found 420.0814.

((*S*)-12-bromo-3-methoxy-9-propoxy-5,8,13,13a-tetrahydro-6H-isoquinolino[3,2-*a*]isoquinoline-2,10-diol) (20b): Yield: 76% (40 mg from 75 mg), light brown solid, mp. 114–118 °C; R_f = 0.42 on silica gel TLC plate in 40:60/EtOAc: Hexanes; ^{1}H NMR (500 MHz, $CDCl_3$): δ 7.02 (s, 1H, ArH), 6.88 (s, 1H, ArH), 6.60 (s, 1H, ArH), 5.56 (brs, 1H), 4.21 (d, *J* = 15.1 Hz, 1H), 3.87 (s, 3H), 3.3.86–3.76 (m, 3H), 3.52 (dd, *J* = 11.2, 4.1 Hz, 1H), 3.45 (d, *J* = 15.1 Hz, 1H), 3.28 (dd, *J* = 16.7, 4.2 Hz, 1H), 3.22–3.11 (m, 2H), 2.70–2.57 (m, 3H), 1.84–1.77 (m, 2H), 1.06 (t, *J* = 7.4 Hz, 3H); ^{13}C NMR (125 MHz, $CDCl_3$): δ 147.4, 145.3, 144.0, 143.3, 129.8, 129.4, 126.4, 125.4, 119.6, 118.8, 111.4, 110.6, 74.7, 59.5, 55.9, 53.8, 51.4, 36.8, 28.7, 23.6, 10.5; HRMS (ESI) *m/z* calcd. for $C_{21}H_{24}BrNO_4$ ([M+H]$^+$), 434.0961, found 434.0963.

((*S*)-12-bromo-9-butoxy-3-methoxy-5,8,13,13a-tetrahydro-6H-isoquinolino[3,2-*a*]isoquinoline-2,10-diol) (20c): Yield: 81% (26 mg from 45 mg), light brown gum; R_f = 0.43 on silica gel TLC plate in 40:60/EtOAc: Hexanes; ^{1}H NMR (500 MHz, $CDCl_3$): δ 6.96 (s, 1H, ArH), 6.88 (s, 1H, ArH), 6.59 (s, 1H, ArH), 4.27 (d, *J* = 15.1 Hz, 1H), 3.87–3.78 (m, 5H), 3.52 (dd, *J* = 11.2, 4.2 Hz, 1H), 3.33 (d, *J* = 15.0 Hz, 1H), 3.26–3.13 (m, 3H), 2.71–2.57 (m, 3H), 1.78–1.68 (m, 2H), 1.56–1.47 (m, 2H), 0.99 (t, *J* = 7.3 Hz, 3H); ^{13}C NMR (125 MHz, $CDCl_3$): δ 147.4, 145.3, 144.1, 143.3, 129.8, 129.4, 126.4, 125.4, 119.7, 118.7, 111.4, 110.6, 72.9, 59.5, 55.9, 53.8, 51.4, 36.8, 32.4, 28.7, 19.2, 13.9; HRMS (ESI) *m/z* calcd. for $C_{22}H_{26}BrNO_4$ ([M+H]$^+$), 448.1118, found 448.1121.

((*S*)-12-bromo-9-butoxy-3-methoxy-5,8,13,13a-tetrahydro-6H-isoquinolino[3,2-*a*]isoquinoline-2,10-diol) (20d): Yield: 61% (22 mg from 50 mg), light brown gum; R_f = 0.41 on silica gel TLC plate in 40:60/EtOAc: Hexanes; ^{1}H NMR (500 MHz, $CDCl_3$): δ 6.97 (s, 1H, ArH), 6.88 (s, 1H, ArH), 6.59 (s, 1H, ArH), 5.63 (brs, 1H), 4.23 (d, *J* = 15.1 Hz, 1H), 3.86 (s, 3H), 3.84–3.81 (m, 2H), 3.52 (dd, *J* = 11.1, 3.8 Hz, 1H), 3.42 (d, *J* = 15.1 Hz, 1H), 3.28–3.12 (m, 3H), 2.71–2.57 (m, 3H), 1.80–1.74 (m, 2H), 1.49–1.36 (m, 4H), 0.94 (t, *J* = 7.1 Hz, 3H); ^{13}C NMR (125 MHz, $CDCl_3$): δ 147.3, 145.2, 144.0, 142.1, 130.1, 129.8, 126.6, 125.7, 119.2, 118.1, 111.4, 110.5, 73.7, 59.3, 55.9, 54.0, 51.3, 37.2, 30.0, 29.0, 28.1, 22.4, 14.0; HRMS (ESI) *m/z* calcd. for $C_{23}H_{28}BrNO_4$ ([M+H]$^+$), 462.1274, found 462.1277.

((*S*)-12-bromo-9-(hexyloxy)-3-methoxy-5,8,13,13a-tetrahydro-6H-isoquinolino[3,2-*a*]isoquinoline-2,10-diol) (20e): Yield: 58% (21 mg from 50 mg), off-white gum; R_f = 0.41 on silica gel TLC plate in 40:60/EtOAc: Hexanes; ^{1}H NMR (500 MHz, $CDCl_3$): δ 6.98 (s, 1H, ArH), 6.88 (s, 1H, ArH), 6.59 (s, 1H, ArH), 5.59 (brs, 1H), 4.22 (d, *J* = 15.1 Hz, 1H), 3.87 (s, 3H), 3.85–3.78 (m, 2H), 3.52 (dd, *J* = 11.2, 4.0 Hz, 1H), 3.42 (d, *J* = 15.1 Hz, 1H), 3.29–3.12 (m, 3H), 2.71–2.57 (m, 3H), 1.79–1.73 (m, 2H), 1.1.50–1.44 (m, 2H), 1.37–1.33 (m, 4H), 0.93–0.90 (m, 3H); ^{13}C NMR (500 MHz, $CDCl_3$): δ 147.3, 145.2, 144.0, 142.8, 130.0, 129.6, 126.5, 125.5, 119.0, 118.9, 111.4, 110.5, 73.4, 59.4, 55.9, 53.9, 51.3, 37.0, 31.6, 30.3, 28.8, 25.6, 22.6, 14.0; HRMS (ESI) *m/z* calcd. for $C_{24}H_{30}BrNO_4$ ([M+H]$^+$), 476.1431, found 476.1447.

((13a*S*)-12-bromo-9-(*sec*-butoxy)-3-methoxy-5,8,13,13a-tetrahydro-6H-isoquinolino[3,2-*a*]isoquinoline-2,10-diol) (20f): Yield: 59% (21 mg from 50 mg), brown gum; R_f = 0.41 on silica gel TLC plate in 40:60/EtOAc: Hexanes; ^{1}H NMR (400 MHz, $CDCl_3$): δ 6.98 (d, *J* = 12.7 Hz, 1H), 6.88 (s, 1H, ArH), 6.59 (s, 1H, ArH), 6.59 (s, 1H, ArH),5.59 (brs, 1H), 4.24–4.19 (m, 1H), 4.06–3.97 (m, 1H), 3.87 (s, 3H), 3.53 (dd, *J* = 11.1, 3.8 Hz, 1H), 3.42–3.37 (m, 1H), 3.29–3.12 (m, 3H), 2.68–2.58 (m, 3H), 1.82–1.71 (m, 1H), 1.69–1.55 (m, 1H), 1.26 (d, *J* = 6.1 Hz, 1.5H), 1.19 (d, *J* = 6.1 Hz, 1.5H), 1.06 (t, *J* = 7.4 Hz, 1.5H), 0.96 (t, *J* = 6.1 Hz, 1.5H); ^{13}C NMR (100 MHz, $CDCl_3$): δ 148.0, 147.8, 145.2, 144.0, 130.1, 130.0, 126.5, 125.5, 118.9, 118.5, 111.4, 110.6, 80.2, 59.5, 55.9, 54.4, 51.4, 37.1, 30.0, 29.1, 19.4, 9.9; HRMS (ESI) *m/z* calcd. for $C_{22}H_{26}BrNO_4$ ([M+H]$^+$), 448.1118, found 448.1118.

((*S*)-12-bromo-3-methoxy-9-(2-methoxyethoxy)-5,8,13,13a-tetrahydro-6H-isoquinolino[3,2-*a*]isoquinoline-2,10-diol) (20g): Yield: 64% (34 mg from 75 mg), brown gum; R_f = 0.41 on silica gel TLC plate in 40:60/EtOAc: Hexanes;^{1}H NMR (400 MHz, $CDCl_3$): δ 8.01 (br. s, 1H), 7.08 (s, 1H, ArH), 6.88 (s, 1H, ArH), 6.59 (s, 1H, ArH), 5.61 (brs, 1H), 4.18 (d, *J* = 15.4 Hz, 1H), 4.12–4.07 (m, 1H), 4.02–3.98 (m, 1H), 3.87 (s, 3H), 3.71–3.67 (m, 2H), 3.53–3.49 (m, 5H), 3.28 (dd, *J* = 16.6, 4.6 Hz, 1H), 3.19–3.09 (m, 2H), 2.69–2.54 (m, 3H); ^{13}C NMR (400 MHz, $CDCl_3$): δ 148.1, 145.1, 143.9, 142.1, 130.3, 130.1, 125.7, 125.5, 119.8, 118.7, 111.4, 110.5, 72.9, 71.5, 59.2, 59.1, 55.9, 54.0, 51.2, 37.1, 29.0; HRMS (ESI) *m/z* calcd. for $C_{21}H_{24}BrNO_5$ ([M+H]$^+$), 450.0911, found 450.0913.

General synthetic procedure for the compounds 22a–22g as demonstrated for 22a: To a stirred solution of compound, **19a** (1.0 eq) in anhydrous THF (8.0 mL) was added *i*-PrMgCl.LiCl (2.0 eq mL), at room temperature. The resulting reaction mixture was allowed to stir for 4–8 h. After completion of the reaction, the reaction was quenched with water and extracted with ethyl acetate (50 mL). The combined organic layer was washed with brine solution and water, dried over Na_2SO_4, and concentrated under reduced pressure. Without further purification the residue (containing compound **21a**) was subjected to the debenzylation procedure as shown for compound **20a** to obtain compound **22a** which was purified by column chromatography on silica gel using 2:98 MeOH:DCM as eluent to afford compound, **22a** as a light yellow gum.

((*S*)-9-ethoxy-3-methoxy-5,8,13,13a-tetrahydro-6H-isoquinolino[3,2-*a*]isoquinoline-2,10-diol) (22a): Yield: 67% (18 mg from 42 mg of **19a**), off-white gum; R_f = 0.38 on silica gel TLC plate in 40:60/EtOAc: Hexanes; ^{1}H NMR (400 MHz, $CDCl_3$): δ 6.80–6.75 (m, 3H, ArH), 6.58 (s, 1H, ArH), 5.61 (brs, 2H), 4.18 (d, *J* = 15.3 Hz, 1H), 4.04–3.89 (m, 2H), 3.86 (s, 3H), 3.55–3.51 (m, 2H), 3.25–3.09 (m, 3H), 2.79 (dd, *J* = 15.6, 11.4 Hz, 1H), 2.69–2.61 (m, 2H), 1.41 (t, *J* = 7.0 Hz, 3H); ^{13}C NMR (100 MHz, $CDCl_3$): δ 146.6, 145.1, 143.9, 142.2, 130.4, 127.9, 127.2, 125.8, 124.7, 114.0, 111.3, 110.5, 69.0, 59.3, 55.8, 54.0, 51.6, 36.0, 29.0, 15.9; HRMS (ESI) *m/z* calcd. for $C_{20}H_{23}NO_4$ ([M+H]$^+$), 342.1700, found 342.1702.

((*S*)-3-methoxy-9-propoxy-5,8,13,13a-tetrahydro-6H-isoquinolino[3,2-*a*]isoquinoline-2,10-diol) (22b): Yield: 72% (19 mg from 40 mg of **19b**), brown gum; R_f = 0.38 on silica gel TLC plate in 40:60/EtOAc: Hexanes; ^{1}H NMR (600 MHz, $CDCl_3$): δ 6.81–6.77 (m, 3H, ArH), 6.60 (s, 1H, ArH), 5.61 (brs, 2H), 4.20 (d, *J* = 15.2 Hz, 1H), 3.90–3.86 (m, 4H), 3.80–3.77 (m, 1H), 3.54 (d, *J* = 14.7 Hz, 2H), 3.26–3.12 (m, 3H), 2.79 (dd, *J* = 15.4, 11.6 Hz, 1H), 2.69–2.62 (m, 2H), 1.86–1.80 (m, 2H), 1.07 (t, *J* = 7.3 Hz, 3H); ^{13}C NMR (150 MHz, $CDCl_3$): δ 146.5, 144.9, 143.7, 142.2, 130.2, 127.8, 127.1, 125.8, 124.7, 113.9, 111.2, 110.4, 74.9, 59.3, 55.8, 53.9, 51.6, 36.0, 29.0, 23.6, 10.4; HRMS (ESI) *m/z* calcd. for $C_{21}H_{25}NO_4$ ([M+H]$^+$), 356.1865, found 356.1865.

((*S*)-9-butoxy-3-methoxy-5,8,13,13a-tetrahydro-6H-isoquinolino[3,2-*a*]isoquinoline-2,10-diol) (22c): Yield: 77% (23 mg from 45 mg of **19c**), light brown gum; R_f = 0.39 on silica gel TLC plate in 40:60/EtOAc: Hexanes; ^{1}H NMR (600 MHz, *CDCl*$_3$): δ 6.79 (s, 1H, ArH) 6.75–6.71 (m, 2H, ArH), 6.58 (s, 1H, ArH), 5.92 (br. s, 2H), 4.21 (d, *J* = 15.2 Hz, 1H), 3.90–3.79 (m, 5H), 3.54–3.49 (m, 2H), 3.23–3.13 (m, 3H), 2.79 (dd, *J* = 15.4, 11.7 Hz, 1H), 2.66 (m, 2H), 1.79–1.74 (m, 2H), 1.53–1.47 (m, 2H), 0.99 (t, *J* = 7.4 Hz, 3H); ^{13}C NMR (150 MHz, $CDCl_3$): δ 146.5, 145.0, 143.8, 142.5, 130.1, 127.6, 127.0, 125.7, 124.6, 114.3, 111.3, 110.4, 73.0, 59.3, 55.7, 53.9, 51.6, 35.8, 28.8, 19.2 × 2, 13.9; HRMS (ESI) *m/z* calcd. for $C_{22}H_{27}NO_4$ ([M+H]$^+$),

370.2013, found 370.2019.

((*S*)-3-methoxy-9-(pentyloxy)-5,8,13,13a-tetrahydro-6H-isoquinolino[3,2-*a*]isoquinoline-2,10-diol) (22d): Yield: 70% (19 mg from 40 mg of **19d**), light brown solid, mp. 86–89 °C; $R_f = 0.38$ on silica gel TLC plate in 40:60/EtOAc: Hexanes; ^{1}H NMR (400 MHz, $CDCl_3$): δ 6.80–6.73 (m, 3H, ArH), 6.58 (s, 1H, ArH), 5.67 (brs, 2H), 4.19 (d, J = 15.3 Hz, 1H), 3.93–3.78 (m, 5H), 3.54–3.50 (m, 2H), 3.24–3.09 (m, 3H), 2.79 (dd, J = 11.4, 15.8 Hz, 1H), 2.70–2.59 (m, 2H), 1.83–1.76 (m, 2H), 1.49–1.34 (m, 4H), 0.94 (t, J = 7.1 Hz, 3H); ^{13}C NMR (100 MHz, $CDCl_3$): δ 146.6, 145.1, 143.9, 142.4, 130.4, 127.8, 127.1, 125.8, 124.6, 114.1, 111.3, 110.5, 73.5, 59.3, 55.8, 54.0, 51.6, 36.0, 30.1, 29.0, 28.1 × 2, 14.0; HRMS (ESI) *m/z* calcd. for $C_{23}H_{29}NO_4$ ($[M+H]^+$), 384.2169, found 384.2172.

((*S*)-9-(hexyloxy)-3-methoxy-5,8,13,13a-tetrahydro-6H-isoquinolino[3,2-*a*]isoquinoline-2,10-diol) (22e): Yield: 76% (26 mg from 50 mg of **19e**), off white gum; $R_f = 0.37$ on silica gel TLC plate in 40:60/EtOAc: Hexanes; ^{1}H NMR (400 MHz, $CDCl_3$): δ 6.80–6.74 (m, 3H, ArH), 6.58 (s, 1H, ArH), 5.61 (brs, 2H), 4.23 (d, J = 15.2 Hz, 1H), 3.93–3.79 (m, 5H), 3.54–3.50 (m, 2H), 3.25–3.09 (m, 3H), 2.79 (dd, J = 11.4, 15.7 Hz, 1H), 2.68–2.59 (m, 2H), 1.82–1.75 (m, 2H), 1.51–1.44 (m, 2H), 1.36–1.33 (m, 4H), 0.93–0.90 (m, 3H); ^{13}C NMR (100 MHz, $CDCl_3$): δ 146.6, 145.1, 143.9, 142.4, 130.4, 127.8, 127.2, 125.8, 124.7, 114.0, 111.3, 110.5, 73.5, 59.3, 55.8, 54.0, 51.6, 36.1, 30.4, 29.1, 25.6, 22.6 × 2, 14.0; HRMS (ESI) *m/z* calcd. for $C_{24}H_{31}NO_4$ ($[M+H]^+$), 398.2326, found 398.2330.

((*S*)-3-methoxy-9-(2-methoxyethoxy)-5,8,13,13a-tetrahydro-6H-isoquinolino[3,2-*a*]isoquinoline-2,10-diol) (22f): Yield: 64% (15 mg from 35 mg of **19f**), off white gum; $R_f = 0.39$ on silica gel TLC plate in 40:60/EtOAc: Hexanes; ^{1}H NMR (400 MHz, $CDCl_3$): δ 6.81–6.78 (m, 3H, ArH), 6.59 (s, 1H, ArH), 5.51 (brs, 1H), 4.18–4.14 (m, 1H), 4.05–4.02 (m, 2H), 3.87 (s, 3H), 3.54–3.49 (m, 2H), 3.27–3.23 (m, 1H), 3.19–3.10 (m, 2H), 2.80 (dd, J = 11.7, 15.4 Hz, 1H), 2.68–2.61 (m, 2H), 1.86–1.77 (m, 1H), 1.70–1.66 (m, 0.5H), 1.61–1.56 (m, 0.5H), 1.31 (d, J = 6.1 Hz, 1.5H), 1.20 (d, J = 6.1 Hz, 1.5H), 1.07 (t, J = 7.4 Hz, 1.5H), 0.97 (t, J = 7.4 Hz, 1.5H); ^{13}C NMR (100 MHz, $CDCl_3$): δ 147.3, 145.0, 143.9, 140.8, 130.6, 128.2, 127.2, 125.8, 124.5, 113.6, 111.3, 110.5, 80.5, 59.4, 55.9, 54.6, 51.7, 36.2, 30.1, 29.4, 19.7, 10.0; HRMS (ESI) *m/z* calcd. for $C_{22}H_{27}NO_4$ ($[M+H]^+$), 3702013, found 370.2020.

((*S*)-3-methoxy-9-(2-methoxyethoxy)-5,8,13,13a-tetrahydro-6H-isoquinolino[3,2-*a*]isoquinoline-2,10-diol) (22g): Yield: 68% (17 mg from 38 mg of **19g**), white solid, mp. 168–172 °C; $R_f = 0.35$ on silica gel TLC plate in 40:60/EtOAc: Hexanes; ^{1}H NMR (400 MHz, $CDCl_3$): δ 7.73 (brs, 1H), 6.83–6.77 (m, 3H, ArH), 6.58 (s, 1H, ArH), 5.62 (brs, 1H), 4.20 (d, J = 15.4 Hz, 1H), 4.12–4.01 (m, 2H), 3.85 (s, 3H), 3.71–3.66 (m, 2H), 3.56–3.49 (m, 5H), 3.23–3.08 (m, 3H), 2.78 (dd, J = 11.4, 15.6 Hz, 1H), 2.68–2.58 (m, 2H); ^{13}C NMR (100 MHz, $CDCl_3$): δ 147.3, 145.1, 143.9, 142.5, 130.5, 128.3, 126.2, 125.9, 125.3, 114.8, 111.4, 110.5, 72.8, 71.6, 59.3, 59.1, 55.8, 54.1, 51.6, 36.1, 29.1; HRMS (ESI) *m/z* calcd for $C_{21}H_{25}NO_5$ ($[M+H]^+$), 372.1805, found 372.1809.

Receptor binding assays: Receptor binding assays were conducted by the PDSP. Details of the assay procedures are available in the online protocol book at the PDSP website (https://pdspdb.unc.edu/pdspWeb/).

Evaluation of potency in interacting with dopamine D_1 and D_3 receptors: The following heterologously expressing cell lines were used: HEK293-rh (rhesus macaque) D_1 and CHO-hD_3. Functional activity of test compounds in activating dopamine (DA) receptors was measured by stimulation of [^{35}S]GTPγS (1250 Ci/mmol, Perkin-Elmer) binding in comparison to stimulation by the full agonist DA as described by us previously [45,46]. With varying DA concentrations starting at 0.1 nM, near-maximal stimulation of GTPγS binding was reached at 1 μM DA for D_1 cells, and 0.1 μM DA for D_3 cells. D_3 DA receptor antagonist activity was assessed by testing a fixed concentration that by itself had little or no effect on baseline [^{35}S]GTPγS binding, for its ability to shift the concentration curve of an agonist stimulating [^{35}S]GTPγS binding as described for opioid receptors by Sally and coworkers [47]. The fixed concentration of compound **22a** was 1 μM. The agonist used was DA (0.1 nM–10 μM). K_e is the functional K_i (equilibrium dissociation constant) of an antagonist and is calculated according to the equation: [Test Compound]/($EC_{50-2}/EC_{50-1} - 1$), where EC_{50-2} is the EC_{50} value in the presence of the test compound and EC_{50-1} is the value in the absence of the test compound.

Acknowledgements

This publication was made possible by Grant Numbers 1SC1GM092282 (WWH), G12MD007599 (WWH), and 5SC3GM095417 (TK) from the National Institutes of Health. Its contents are solely the responsibility of the authors and do not necessarily represent the official views of the NIH or its divisions. K_i determinations, and receptor binding profiles were generously provided by the National Institute of Mental Health's Psychoactive Drug Screening Program, Contract # HHSN-271-2008-00025-C (NIMH PDSP). The NIMH PDSP is directed by Bryan L. Roth MD, PhD at the University of North Carolina at Chapel Hill and Project Officer Jamie Driscol at NIMH, Bethesda MD, USA. For experimental details please refer to the PDSP website http://pdsp.med.unc.edu/ and click on “Binding Assay” or “Functional Assay” on the menu bar. We are grateful to Dr. K. Neve, Oregon Health and Science University, Portland, OR, for rhesus macaque D_1 dopamine receptor expressing HEK293 cells. We thank Tamara Antonio for expert execution of the dopamine receptor assays with GTPγ-S.

Appendix A. Supplementary data

Supplementary data related to this article can be found at http://dx.doi.org/10.1016/j.ejmech.2016.09.036.

References

[1] W. Qian, W. Lu, H. Sun, Z. Li, L. Zhu, R. Zhao, L. Zhang, S. Zhou, Y. Zhou, H. Jiang, X. Zhen, H. Liu, Design, synthesis, and pharmacological evaluation of novel tetrahydroprotoberberine derivatives: selective inhibitors of dopamine D(1) receptor, Bioorg. Med. Chem. 20 (2012) 4862–4871.

[2] H. Sun, L. Zhu, H. Yang, W. Qian, L. Guo, S. Zhou, B. Gao, Z. Li, Y. Zhou, H. Jiang, K. Chen, X. Zhen, H. Liu, Asymmetric total synthesis and identification of tetrahydroprotoberberine derivatives as new antipsychotic agents possessing a dopamine D(1), D(2) and serotonin 5-HT(1A) multi-action profile, Bioorg. Med. Chem. 21 (2013) 856–868.

[3] B. Ma, K. Yue, L. Chen, X. Tian, Q. Ru, Y. Gan, D. Wang, G. Jin, C. Li, L-stepholidine, a natural dopamine receptor D1 agonist and D2 antagonist, inhibits heroin-induced reinstatement, Neurosci. Lett. 559 (2014) 67–71.

[4] J.R. Hao, N. Sun, L. Lei, X.Y. Li, B. Yao, K. Sun, R. Hu, X. Zhang, X.D. Shi, C. Gao, L-Stepholidine rescues memory deficit and synaptic plasticity in models of Alzheimer's disease via activating dopamine D1 receptor/PKA signaling pathway, Cell Death Dis. 6 (2015) e1965.

[5] K. Yue, B. Ma, L. Chen, X. Tian, Q. Ru, Y. Gan, D. Wang, G. Jin, C. Li, L-Stepholidine, a naturally occurring dopamine D1 receptor agonist and D2 receptor antagonist, attenuates heroin self-administration and cue-induced reinstatement in rats, Neuroreport 25 (2014) 7–11.

[6] J. Mo, H. Zhang, L.P. Yu, P.H. Sun, G.Z. Jin, X. Zhen, L-stepholidine reduced L-DOPA-induced dyskinesia in 6-OHDA-lesioned rat model of Parkinson's disease, Neurobiol. Aging 31 (2010) 926–936.

[7] S. Natesan, G.E. Reckless, K.B. Barlow, J. Odontiadis, J.N. Nobrega, G.B. Baker, S.R. George, D. Mamo, S. Kapur, The antipsychotic potential of l-stepholidine–a naturally occurring dopamine receptor D1 agonist and D2 antagonist, Psychopharmacology 199 (2008) 275–289.

[8] H. Chu, G. Jin, E. Friedman, X. Zhen, Recent development in studies of tetrahydroprotoberberines: mechanism in antinociception and drug addiction, Cell. Mol. Neurobiol. 28 (2008) 491–499.

[9] K. Yang, G. Jin, J. Wu, The neuropharmacology of (-)-stepholidine and its potential applications, Curr. Neuropharmacol. 5 (2007) 289–294.

[10] W. Wang, Y. Zhou, J. Sun, L. Pan, L. Kang, Z. Dai, R. Yu, G. Jin, L. Ma, The effect of L-stepholidine, a novel extract of Chinese herb, on the acquisition, expression, maintenance, and re-acquisition of morphine conditioned place preference in

rats, Neuropharmacology 52 (2007) 355–361.
[11] J. Mo, Y. Guo, Y.S. Yang, J.S. Shen, G.Z. Jin, X. Zhen, Recent developments in studies of l-stepholidine and its analogs: chemistry, pharmacology and clinical implications, Curr. Med. Chem. 14 (2007) 2996–3002.
[12] B.A. Ellenbroek, X.X. Zhang, G.Z. Jin, Effects of (-)stepholidine in animal models for schizophrenia, Acta Pharmacol. Sin. 27 (2006) 1111–1118.
[13] W. Xu, Y. Wang, Z. Ma, Y.T. Chiu, P. Huang, K. Rasakham, E. Unterwald, D.Y. Lee, L.Y. Liu-Chen, L-isocorypalmine reduces behavioral sensitization and rewarding effects of cocaine in mice by acting on dopamine receptors, Drug Alcohol Depend. 133 (2013) 693–703.
[14] S. Sushchyk, Z.X. Xi, J.B. Wang, Combination of levo-tetrahydropalmatine and low dose naltrexone: a promising treatment for prevention of cocaine relapse, J. Pharmacol. Exp. Ther. 357 (2016) 248–257.
[15] T. Kim, D.J. Hinton, S. Johng, J.B. Wang, D.S. Choi, Levo-tetrahydropalmatine decreases ethanol drinking and antagonizes dopamine D2 receptor-mediated signaling in the mouse dorsal striatum, Behav. Brain Res. 244 (2013) 58–65.
[16] J.B. Wang, J.R. Mantsch, l-tetrahydropalamatine: a potential new medication for the treatment of cocaine addiction, Future Med. Chem. 4 (2012) 177–186.
[17] Y. Figueroa-Guzman, C. Mueller, O. Vranjkovic, S. Wisniewski, Z. Yang, S.J. Li, C. Bohr, E.N. Graf, D.A. Baker, J.R. Mantsch, Oral administration of levo-tetrahydropalmatine attenuates reinstatement of extinguished cocaine seeking by cocaine, stress or drug-associated cues in rats, Drug Alcohol Depend. 116 (2011) 72–79.
[18] J.R. Mantsch, S. Wisniewski, O. Vranjkovic, C. Peters, A. Becker, A. Valentine, S.J. Li, D.A. Baker, Z. Yang, Levo-tetrahydropalmatine attenuates cocaine self-administration under a progressive-ratio schedule and cocaine discrimination in rats, Pharmacol. Biochem. Behav. 97 (2010) 310–316.
[19] Z.X. Xi, Z. Yang, S.J. Li, X. Li, C. Dillon, X.Q. Peng, K. Spiller, E.L. Gardner, Levo-tetrahydropalmatine inhibits cocaine's rewarding effects: experiments with self-administration and brain-stimulation reward in rats, Neuropharmacology 53 (2007) 771–782.
[20] J.R. Mantsch, S.J. Li, R. Risinger, S. Awad, E. Katz, D.A. Baker, Z. Yang, Levo-tetrahydropalmatine attenuates cocaine self-administration and cocaine-induced reinstatement in rats, Psychopharmacology 192 (2007) 581–591.
[21] B.R. Lins, A.G. Phillips, J.G. Howland, Effects of D- and L-govadine on the disruption of touchscreen object-location paired associates learning in rats by acute MK-801 treatment, Psychopharmacology 232 (2015) 4371–4382.
[22] D.M. Ashby, C.C. Lapish, A.G. Phillips, Stability of avoidance behaviour following repeated intermittent treatment with clozapine, olanzapine or D,L-govadine, Behav. Pharmacol. 26 (2015) 133–138.
[23] C.C. Lapish, K.C. Ahn, R.A. Chambers, D.M. Ashby, S. Ahn, A.G. Phillips, Selective effects of D- and L-govadine in preclinical tests of positive, negative, and cognitive symptoms of schizophrenia, Neuropsychopharmacol. Off. Publ. Am. Coll. Neuropsychopharmacol. 39 (2014) 1754–1762.
[24] C.C. Lapish, F. Belardetti, D.M. Ashby, S. Ahn, K.A. Butts, K. So, C.M. Macrae, J.J. Hynd, J.J. Miller, A.G. Phillips, A preclinical assessment of d.l-govadine as a potential antipsychotic and cognitive enhancer, Int. J. Neuropsychopharmacol./Off. Sci. J. Coll. Int. Neuropsychopharmacol. 15 (2012) 1441–1455.
[25] Z.H. Liu, W.Q. Jin, H.P. Zhang, X.J. Chen, G.Z. Jin, Suppression of morphine-induced conditioned place preference by l-12-chloroscoulerine, a novel dopamine receptor ligand, Pharmacol. Biochem. Behav. 75 (2003) 289–294.
[26] Y. He, W.Q. Jin, Q.X. Shen, X.J. Chen, G.Z. Jin, Expression of dopamine D1 receptor in Sf9 insect cells and agonism of l-12-chloroscoulerine on recombinant D1 receptor, Acta Pharmacol. Sin. 24 (2003) 225–229.
[27] L.J. Chen, Q.T. Zhou, Z.J. Dong, L.P. Yu, G.Z. Jin, Comparison of 12-chloroscoulerine enantiomers on animal behavior to dopamine receptors, Zhongguo Yao Li Xue Bao = Acta Pharmacol. Sin. 20 (1999) 884–888.
[28] J. Parraga, N. Cabedo, S. Andujar, L. Piqueras, L. Moreno, A. Galan, E. Angelina, R.D. Enriz, M.D. Ivorra, M.J. Sanz, D. Cortes, 2,3,9- and 2,3,11-trisubstituted tetrahydroprotoberberines as D2 dopaminergic ligands, Eur. J. Med. Chem. 68 (2013) 150–166.
[29] G.Z. Jin, X.L. Wang, W.X. Shi, Tetrahydroprotoberberine–a new chemical type of antagonist of dopamine receptors, Sci. Sin. Ser. B Chem. Biol. Agric. Med. Earth Sci./Chung-kuo k'o Hsueh Yuan Chu Pan 29 (1986) 527–534.
[30] D. Cortes, J. Arbaoui, P. Protais, High affinity and selectivity of some tetrahydroprotoberberine alkaloids for rat striatal 3H-raclopride binding sites, Nat. Prod. Lett. 3 (1993) 233–238.
[31] S. Gadhiya, S. Madapa, T. Kurtzman, I.L. Alberts, S. Ramsey, N.K. Pillarsetty, T. Kalidindi, W.W. Harding, Tetrahydroprotoberberine alkaloids with dopamine and sigma receptor affinity, Bioorg. Med. Chem. 24 (2016) 2060–2071.
[32] R. Wilcken, M.O. Zimmermann, A. Lange, A.C. Joerger, F.M. Boeckler, Principles and applications of halogen bonding in medicinal chemistry and chemical biology, J. Med. Chem. 56 (2013) 1363–1388.
[33] D.S. Bhakuni, P. Kumar, Studies on Mannich reaction of 1-benzyltetrahydroisoquinolines, J. Indian Chem. Soc. 65 (1988) 417–421.
[34] N. Cabedo, I. Berenguer, B. Figadere, D. Cortes, An overview on benzylisoquinoline derivatives with dopaminergic and serotonergic activities, Curr. Med. Chem. 16 (2009) 2441–2467.
[35] E.Y. Chien, W. Liu, Q. Zhao, V. Katritch, G.W. Han, M.A. Hanson, L. Shi, A.H. Newman, J.A. Javitch, V. Cherezov, R.C. Stevens, Structure of the human dopamine D3 receptor in complex with a D2/D3 selective antagonist, Science 330 (2010) 1091–1095.
[36] H.M. Berman, J. Westbrook, Z. Feng, G. Gilliland, T.N. Bhat, H. Weissig, I.N. Shindyalov, P.E. Bourne, The protein Data Bank, Nucleic Acids Res. 28 (2000) 235–242.
[37] G.M. Sastry, M. Adzhigirey, T. Day, R. Annabhimoju, W. Sherman, Protein and ligand preparation: parameters, protocols, and influence on virtual screening enrichments, J. Comput. Aided Mol. Des. 27 (2013) 221–234.
[38] R.A. Friesner, J.L. Banks, R.B. Murphy, T.A. Halgren, J.J. Klicic, D.T. Mainz, M.P. Repasky, E.H. Knoll, M. Shelley, J.K. Perry, D.E. Shaw, P. Francis, P.S. Shenkin, Glide: a new approach for rapid, accurate docking and scoring. 1. Method and assessment of docking accuracy, J. Med. Chem. 47 (2004) 1739–1749.
[39] E. Harder, W. Damm, J. Maple, C. Wu, M. Reboul, J.Y. Xiang, L. Wang, D. Lupyan, M.K. Dahlgren, J.L. Knight, J.W. Kaus, D.S. Cerutti, G. Krilov, W.L. Jorgensen, R. Abel, R.A. Friesner, OPLS3: a force field providing broad coverage of drug-like small molecules and proteins, J. Chem. Theory Comput. 12 (2016) 281–296.
[40] P. Politzer, P. Lane, M.C. Concha, Y. Ma, J.S. Murray, An overview of halogen bonding, J. Mol. Model. 13 (2007) 305–311.
[41] M.R. Scholfield, C.M. Zanden, M. Carter, P.S. Ho, Halogen bonding (X-bonding): a biological perspective, Protein Sci. Publ. Protein Soc. 22 (2013) 139–152.
[42] H.W. Horn, W.C. Swope, J.W. Pitera, J.D. Madura, T.J. Dick, G.L. Hura, T. Head-Gordon, Development of an improved four-site water model for biomolecular simulations: TIP4P-Ew, J. Chem. Phys. 120 (2004) 9665–9678.
[43] J.A. Maier, C. Martinez, K. Kasavajhala, L. Wickstrom, K.E. Hauser, C. Simmerling, ff14SB: improving the accuracy of protein side chain and backbone parameters from ff99SB, J. Chem. Theory Comput. 11 (2015) 3696–3713.
[44] J. Wang, R.M. Wolf, J.W. Caldwell, P.A. Kollman, D.A. Case, Development and testing of a general amber force field, J. Comput. Chem. 25 (2004) 1157–1174.
[45] B. Das, S. Vedachalam, D. Luo, T. Antonio, M.E. Reith, A.K. Dutta, Development of a highly potent D2/D3 agonist and a partial agonist from structure-activity relationship study of N(6)-(2-(4-(1H-Indol-5-yl)piperazin-1-yl)ethyl)-N(6)-propyl-4,5,6,7-tetrahydroben zo[d]thiazole-2,6-diamine analogues: implication in the treatment of Parkinson's disease, J. Med. Chem. 58 (2015) 9179–9195.
[46] B. Ghosh, T. Antonio, B. Gopishetty, M. Reith, A. Dutta, Further delineation of hydrophobic binding sites in dopamine D(2)/D(3) receptors for N-4 substituents on the piperazine ring of the hybrid template 5/7-{[2-(4-aryl-piperazin-1-yl)-ethyl]-propyl-amino}-5,6,7,8-tetrahydro-naphthale n-2-ol, Bioorg. Med. Chem. 18 (2010) 5661–5674.
[47] E.J. Sally, H. Xu, C.M. Dersch, L.W. Hsin, L.T. Chang, T.E. Prisinzano, D.S. Simpson, D. Giuvelis, K.C. Rice, A.E. Jacobson, K. Cheng, E.J. Bilsky, R.B. Rothman, Identification of a novel “almost neutral” micro-opioid receptor antagonist in CHO cells expressing the cloned human mu-opioid receptor, Synapse 64 (2010) 280–288.